Co-funded by the
Erasmus+ Programme
of the European Union

Innovative Teaching Approaches in development of Software Designed Instrumentation and its application in real-time systems
Erasmus+ KA2 strategic partnership

Seminar on measurement and data acquisition

STUDENT POSTER SESSION

University of Belgrade - School of Electrical Engineering
Innovation Center, School of Electrical Engineering - University of Belgrade
25th October 2019, Belgrade, Serbia

ITASDI partners

http://itasdi.uns.ac.rs

Industry representatives

The European Commission's support for the production of this publication does not constitute an endorsement of the contents, which reflect the views only of the authors, and the Commission cannot be held responsible for any use which may be made of the information contained therein.

COMPUTER VISION BASED OBJECT TRACKING USING 2-DOF GIMBAL

Savo Ičagić

University of Belgrade, School of Electrical Engineering
Signals & Systems Department

Abstract: **Design and operation of cheap and robust real-time visual object tracking system is described in this paper. Task of this system is to keep object at centre of the frame by aiming camera in real-time by pan/tilt mechanism. Software for image processing is written using OpenCV (Intel Corporation, Santa Clara, USA) computer vision library. Digital controller is based on Arduino (Somerville, USA) platform. Results of this project can be used as reliable platform in further research and development in object tracking/localization applications or development of autonomous weapons platform.**

Keywords **- Arduino, computer vision, OpenCV, visual object tracking**

Introduction

Computer vision is important field of research in key aspects of modern day technology (artificial intelligence, autonomous vehicles, robotics etc.) which are considered to be protagonists of Fourth industrial revolution [1]. Object tracking is one of fundamental components of computer vision.
Object tracking is vital in many aspects of life: in parts of multisensor object tracking systems of autonomous cars [3], in CCTV systems etc. Real-time face recognition, tracking and identification is growing field of application of these technologies in effort to monitor persons of interest [4]. Besides tracking macroscopic objects, visual object tracking is also used in tracking of microscopic objects, such as microorganisms [5].
Goal of this poster is realization of cheap and robust hardware and software platform which can be used in further research and development in field of visual object tracking.

Methodology

Object tracking software is written in *Python* (*Python Software Foundation*, Delaware, USA) based on *OpenCV* (Intel Corporation, Santa Clara, USA) computer vision library and executed on PC. Block diagram of system is given in Figure 1.

Task of digital controller is to parse control values from object tracking software and to power stepper motors accordingly. Digital controller is based on *Arduino Nano* (Somerville, USA) board. Firmware is written in C/C++, in a form of finite state machine (FSM). Commands are received from PC object tracking software in form of ASCII string: "{t_{pan};t_{tilt}}", t_{pan} and t_{tilt} are integer control values which describe speed of motors. Block diagram of digital controller is given in Figure 2.

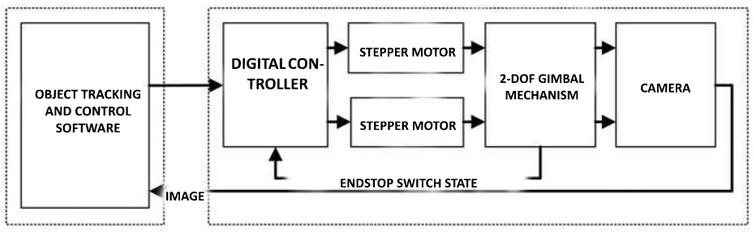

Figure 1
Block diagram of object tracking system

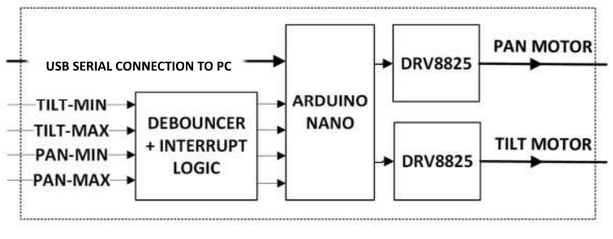

Figure 2
Block diagram of digital controller

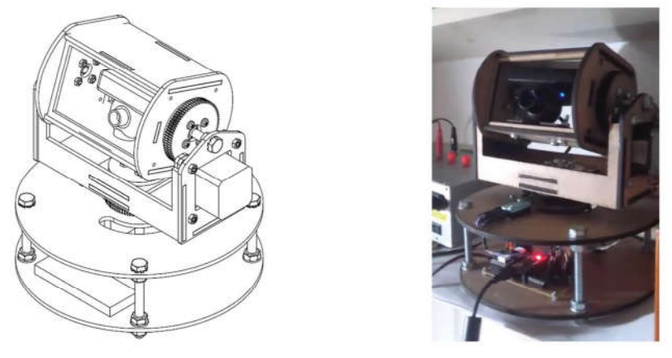

Figure 3
Photo of gimbal (left) and CAD drawing of gimbal (right)

Two methods of object tracking are implemented - tracking of color marker and tracking of any object in frame.
Tracking of color marker is actually tracking by detection - in each frame biggest blob of specific color is detected and considered for object being tracked.
Screenshot with individual steps of image processing is given in Figure 4. Algorithm is given in Figure 5 (right). Example of tracking colored object is given in Fig.6 (top right).
Tracking of selected object in frame is implemented using KCF tracker from OpenCV library. Algorithm is given in Figure 5 (left). Example of face tracking is given in Fig.6 (bottom).

Gimbal is custom made from laser cut 4mm MDF boards, and uses NEMA 17 stepper motors for axis actuation (Figure 3 left and right). CAD is used in gimbal design with design goal defined as "no extra machining is required besides laser cutting".
In this particular case, controller has a task to keep tracked object in centre of frame. Coordinate system is defined in Figure 6 (top left). Error signals are $\Delta x(t)$, $\Delta y(t)$ and they are equal to position of object in previously defined coordinate system. Gimbal axis are orthogonal which means, in this particular scenario, system is decoupled. This fact enables use of simple PID controllers for each axis.

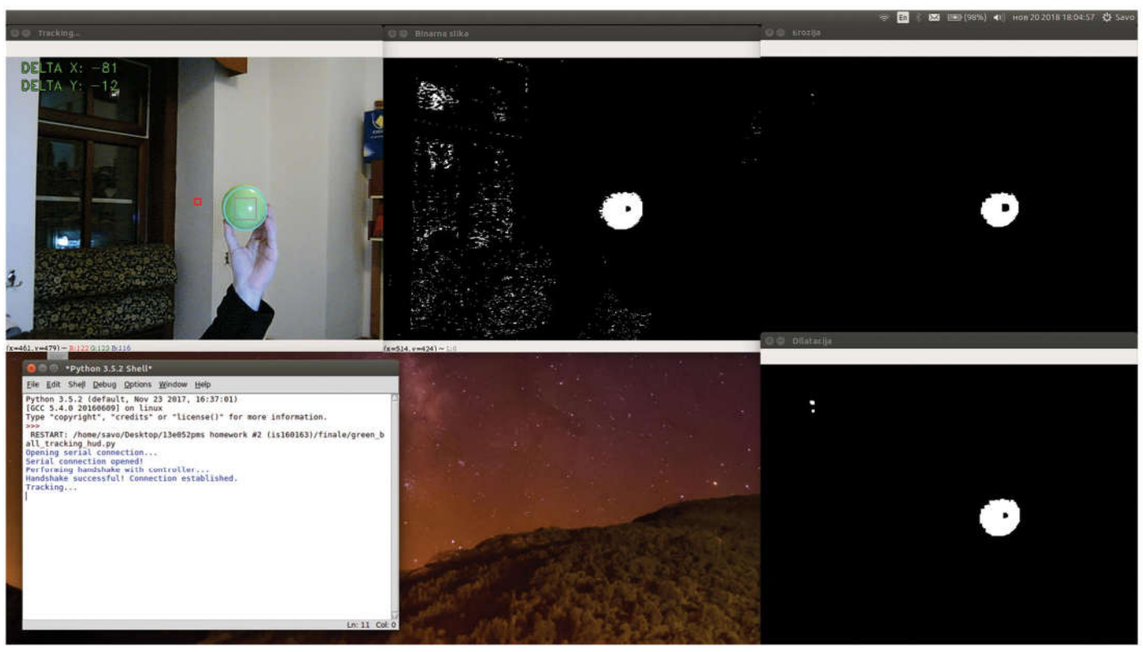

Figure 4 - from top left corner CW: raw input frame, binary image with green isolated, image erosion result, image dilatation result

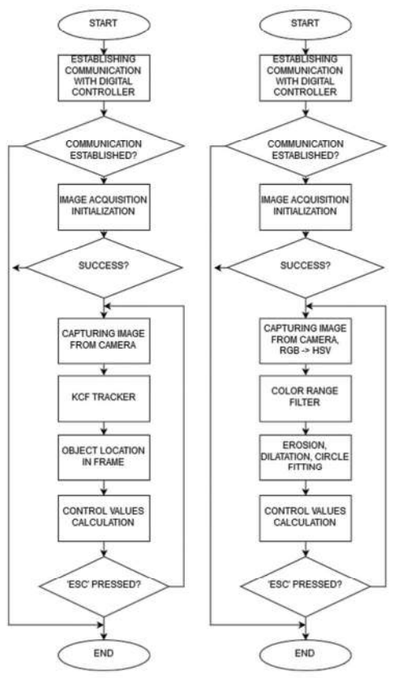

Figure 5 - Program flowchart: tracking by detection (right), and tracking using KCF tracker (left)

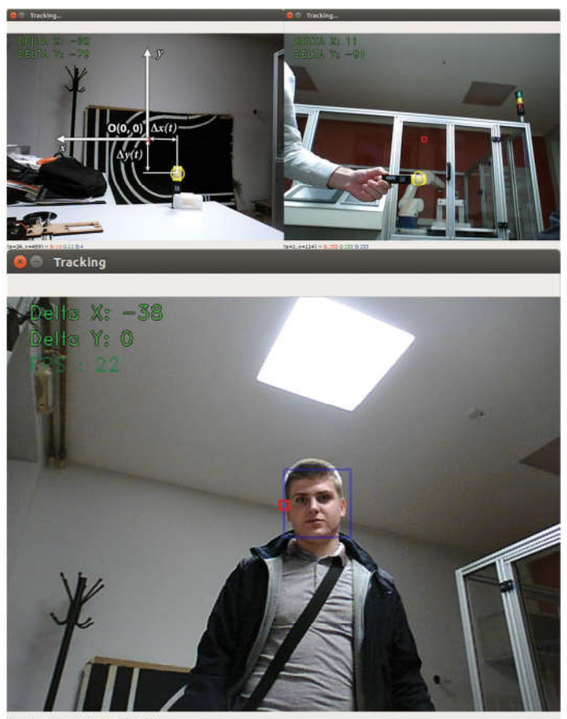

Figure 6 - from top left CW: reference coordinate system, tracking of colored object and tracking of selected face in frame

Conclusion

Hardware platform is robust and it is able to withstand additional load in future upgrades. Software is object oriented which enables simple reuse and upgrade of code.
Simple algorithm of tracking color marker turned out to be robust method and resulted high framerate, enabling tracking of fast moving objects.
Tracking using KCF tracker from OpenCV library turned out to be less robust method than previous method. When an object becomes to similar to background KCF tracker tends to lose track of it. In terms of performance, with increase of size of tracked object in frame - CPU load increases significantly which leads to low framerate. Low framerate effectively increases period of control loop and once valid PID parameters are no longer useful, and system tends to oscillate.
Future use of this platform is versatile. It can be used wherever 2-DoF gimbal with visual object tracking is needed, for example autonomous weapon platform, aiming directional antenna towards some object in the sky (high altitude balloons, long range drones, satellites etc.). [6]

Acknowledgements

I am thankful to lecturers on undergraduate course Practicum of measurement and data acquisition systems for providing opportunity to work on interesting project like this.

Literature

[1] K. Schwab, The Fourth Industrial Revolution, New York: Crown Business, 2017
[2] I. Nesnas, M. Bajracharya, R.Madison, E. Bandari, C. Kunz, M. Deans, M. Bualat „Visual Target Tracking for Rover-based Planetary Exploration", 2004 IEEE Aerospace Conference Proceedings, volume: 6, March 2004
[3] H. Cho, Y. Seo, B.V.K. Vijaya Kumar, R. Rajkumar „A Multi-Sensor Fusion System for Moving Object Detection and Tracking in Urban Driving Environments", 2014 IEEE Int. Conf. on Robotics & Automation (ICRA), June 2014
[4] J. Woodward, C. Horn, J. Gatune, A. Thomas „Biometrics: A Look at Facial Recognition", RAND Corporation, Santa Monica, CA, 2003
[5] N. Ogawa,, H. Oku, K. Hashimoto, M. Ishikawa „Microrobotic Visual Control of Motile Cells Using High-Speed Tracking System" IEEE TRANSACTIONS ON ROBOTICS, volume: 21 , issue: 4 , pp. 704 – 712, Aug. 2005
[6] S. Ičagić, "Real-time visual object tracking system", presented at 26th Telecommunications Forum TELFOR 2018, Belgrade, Serbia, November 20-21, 2018

System for quantitative assessment of finger dexterity from contact force measurements

Milica Badža[1,2]
[1]University of Belgrade - School of Electrical Engineering
[2]Innovation Center, School of Electrical Engineering, University of Belgrade

INTRODUCTION - Hand movements, particullary fingers, are frequently affected after a disease. Exercise and rehabilitation are an effective type of intervention, but progress is slow and invisible to the human eye. Having a sensor system which could be used for objective assessment of our motor performance and potential impairments can help clinicians to track small and slow changes in the recovery.
In this paper, we propose a novel system for measuring finger force profiles for dexterity assessment. The system was introduced as part of the work at the 26th Telecommunications Forum TELFOR 2018 [1] and the journal [2].

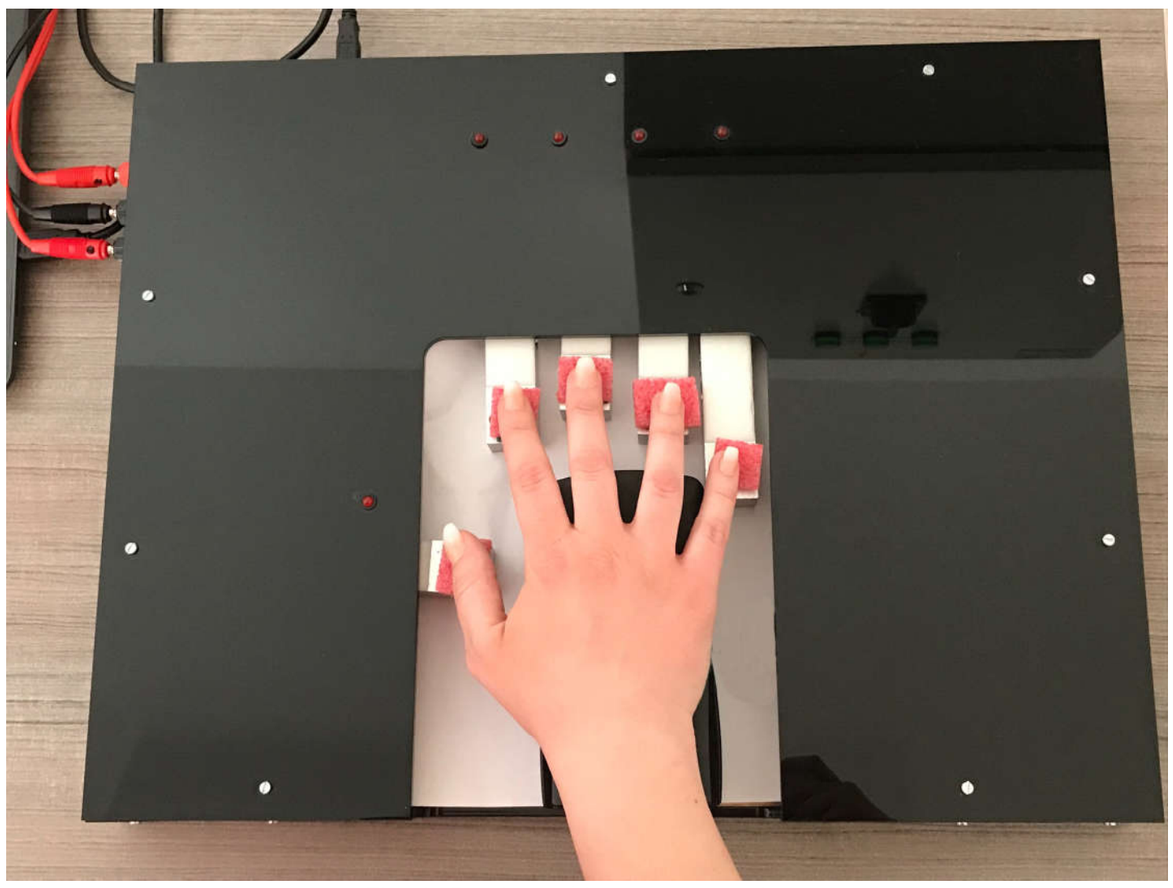

Fig. 1. Designed instrumentation.

METHOD - A system consisting of a software application and hardware assembled into a suitable PVC casing adapted to the anatomy of the left and right hands, separately, was implemented. The developed application controls turning ON/OFF of the LEDs (each LED corresponds to one finger) to signalize the user which finger should press the corresponding strain gage force sensor. The user-friendly application is developed in LabVIEW ver. 2017 environment (National Instruments Inc., Austin, USA).

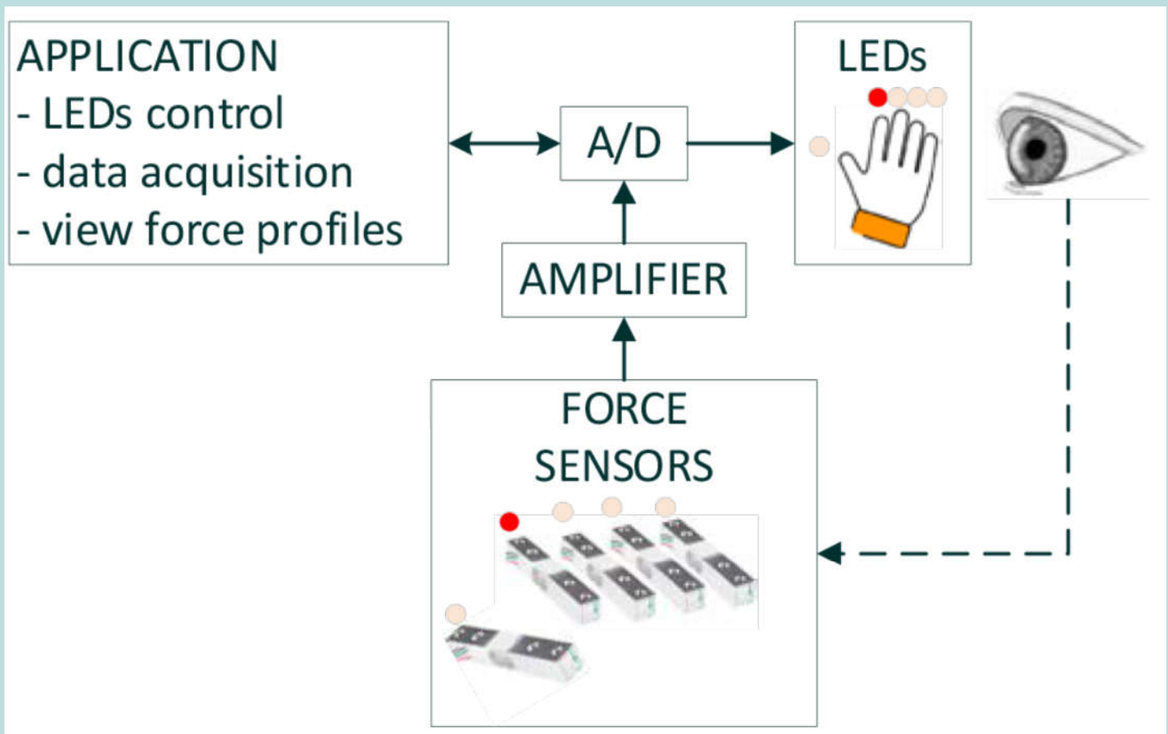

Fig. 2. The block diagram for the right-hand part of the system.

During testing, data are collected as force profiles and characteristic parameters are calculated.
The potential usage of the system is illustrated through an experiment example on four healthy subjects.

RESULTS - Statistical analysis was performed using the software environment R ver. 3.5.1, Foundation for Statistical Computing. The mean value and the standard deviation were calculated for the previously listed response parameters. The force profiles of all trials were aligned to the peak, averaged and shifted to the mean value of the time reaction in order to better visualize the obtained data. Such force profiles of all subjects were further averaged using the same procedure.

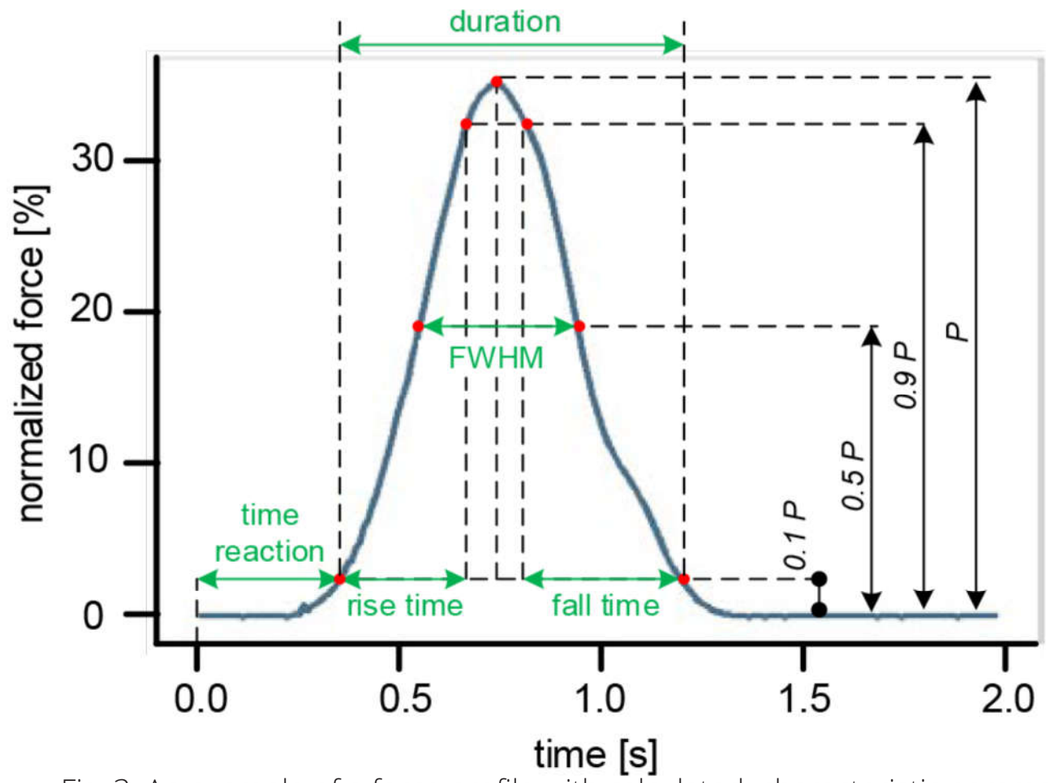

Fig. 3. An example of a force profile with calculated characteristic parameters.

Table 1. Mean value ± standard deviation for all parameters for the averaged profiles of all subjects, shown according to the fingers of the right and left hands.

Parameters	Thumb		Index		Middle		Ring		Little	
	Right	Left	Right	Left	Right	Left	Right	Left	Right	Left
RT [ms]	112± 27	117± 27	97± 27	100± 26	97± 26	105± 30	110± 32	115± 30	120± 35	120± 34
FT [ms]	77± 13	90± 16	72± 9	82± 15	70± 8	80± 12	80± 14	87± 13	85± 19	75± 13
P [%]	43± 19	15± 4	34± 15	29± 8	31± 19	29± 14	31± 15	36± 27	39± 18	33± 17
D [ms]	245± 47	265± 46	220± 49	235± 49	215± 40	230± 49	242± 53	257± 51	257± 64	245± 58
TR [ms]	512± 74	530± 75	477± 60	430± 35	505± 38	492± 62	520± 81	475± 26	455± 52	447± 48
FWHM [ms]	147± 26	152± 29	132± 31	140± 15	122± 21	133± 22	140± 22	150± 22	152± 34	148± 32

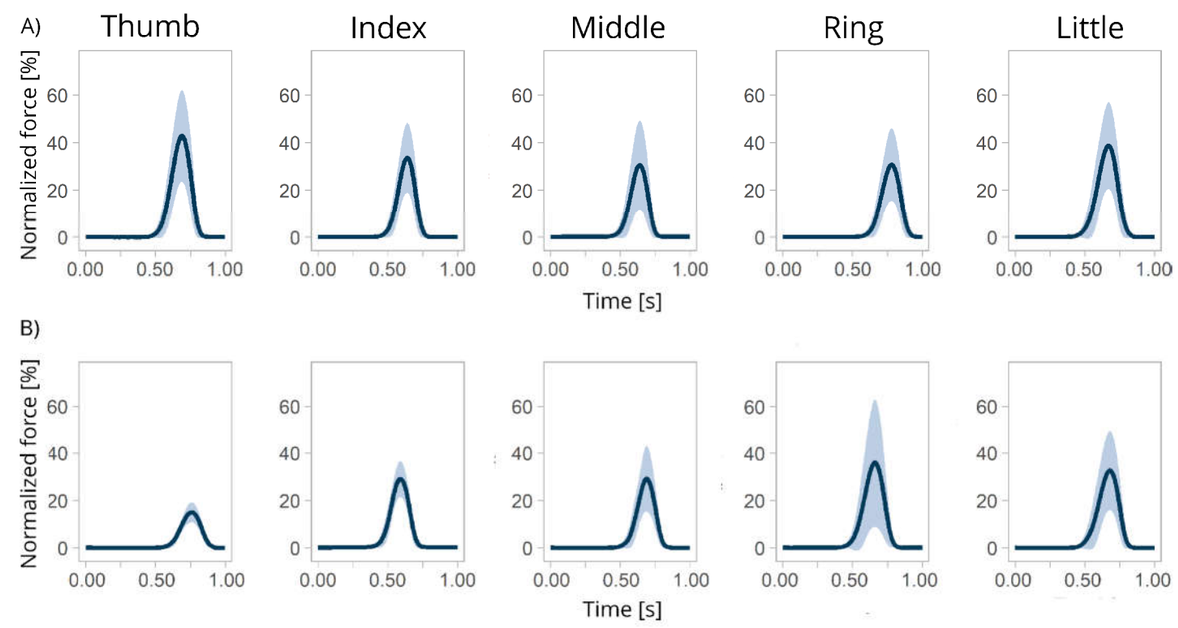

Fig. 4. Aligned and averaged force profiles for all subjects for: A) right and B) left hand.

CONCLUSION - The relative error of standard deviations for calculated parameters, except for peak of force, is in the range 6-28%. Parameters *TR, RT*, and *FT* were approximately the same for all subjects. The shape of the finger force profile is similar for all fingers for both hands. The peak of the force shows the highest variability, both for the finger itself and between the fingers and hands.
In addition to the shape of the force profile itself, the parameters *TR, D* and *FWHM* can serve as an indication of normal finger mobility.
By using the developed system it is possible to track small and slow changes in finger movements. The system is encased and functions on a plug-and-play principle which makes it easy to use in clinics.

LITERATURE

[1] M. M. Badza, M. M. Novicic, M. Duric-Jovicic, M. M. Jankovic, and M. B. Popovic, "System for Measuring Finger Force Profiles for Dexterity Assessment," in 2018 26th Telecommunications Forum, TELFOR 2018 - Proceedings, 2019.
[2] M. Badža, M. Novičić, M. Djurić-Jovičić, M. M. Jankovic, and M. Popović, "System for Measuring Finger Force Profiles for Dexterity Assessment," Telfor J., 2019, accepted.

Validation of a camera based gait analysis system

Ivan Vajs[1,2]

[1]University of Belgrade – School of Electrical Engineering
[2]Innovation Center, University of Belgrade - School of Electrical Engineering

Fig 1. Systems for gait analysis: inertial units (left) and optical system (right).

Introduction

Human gait is a complex form of movement that requires the coordination of the nervous and muscular system. Clinicians often observe this type of motion in order to assess the state of a patient during the recovery process or in order to make a certain diagnosis. Many systems for objective gait analysis which can describe the movement using different parameters have been developed. These systems ensure objective decision making and quantitative measurements that can easily be compared.

This paper describes a developed camera based gait analysis system that consists of handmade optical markers and two smartphone cameras. The developed system is used to track angles of thighs and shanks on both legs and it was validated by an established system of inertial measurement units – Mtw Awinda.

Experiment

There were four subjects that participated in the experiment. Each of them was instructed to walk on a treadmill at 2 km/h and 3 km/h and to jog at 4 km/h. Each recording session consisted of one subject moving at one fixed speed for about 2 minutes. During the session the angles of thighs and shanks of both legs in the sagittal plane were measured by the two systems. All the subjects were healthy with ages ranging from 22 to 32.

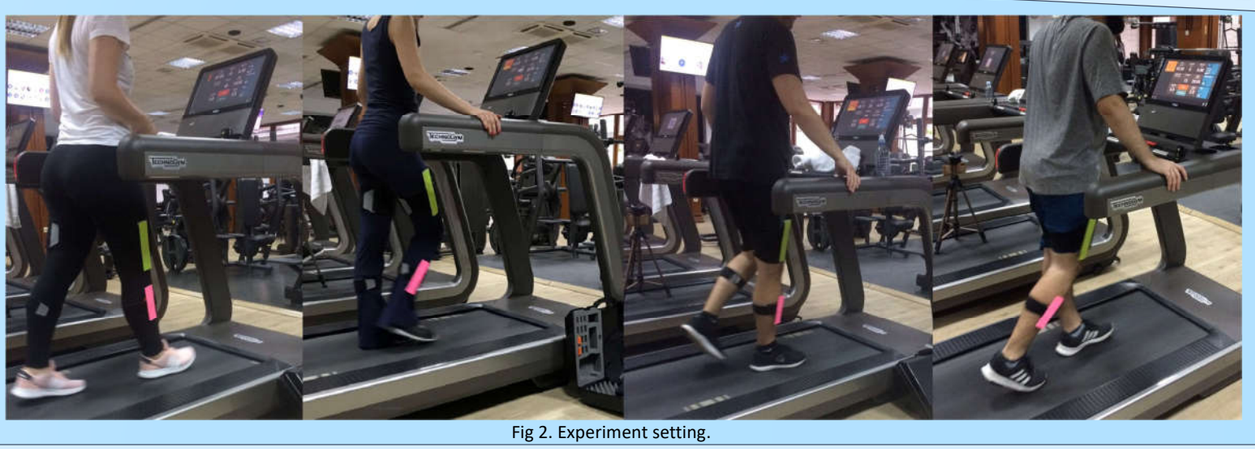

Fig 2. Experiment setting.

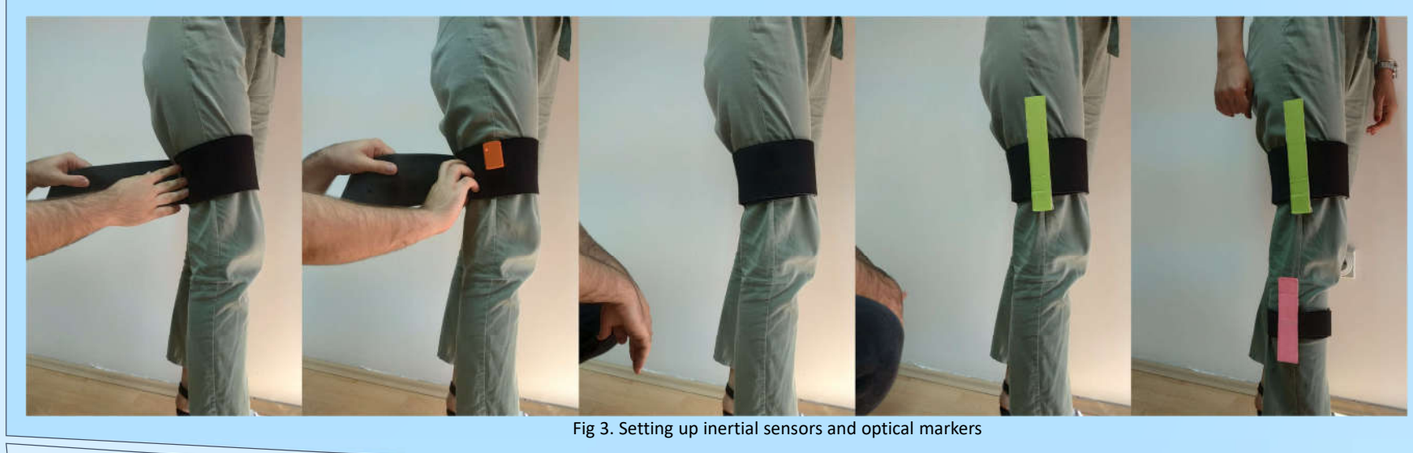

Fig 3. Setting up inertial sensors and optical markers

Instrumentation

The system that was used for reference in the validation process consists of four inertial measurement units and a wireless communication station. Each of the sensors is placed on the corresponding leg segment using velcro tape. The system that was being validated used four optical markers (each for one leg segment) and two smartphone cameras. The markers were placed on the on the velcro tape, above the previously positioned sensors. The two cameras were placed on each side of the treadmill so that they could record the movement of the subject's lower extremities.

Video processing

In order to obtain the sagittal plane angles of each body segment image processing is performed. One frame from a single camera contains information about the orientation of the shank and the thigh of the corresponding leg. The color components of each pixel in the frame are compared to threshold values and among themselves in order to separate the area of the thigh and shank markers respectively. Once the marker of a leg segment is separated from the rest of the image, the orientation of the blob that represents the marker can be calculated. This orientation describes the angle of the corresponding leg segment in the sagittal plane at the moment the frame was captured. By repeating the process for all the frames of the two videos (one for the left leg and one for the right leg), a sequence of angles is obtained for each observed leg segment that represent its movement in the sagittal plane.

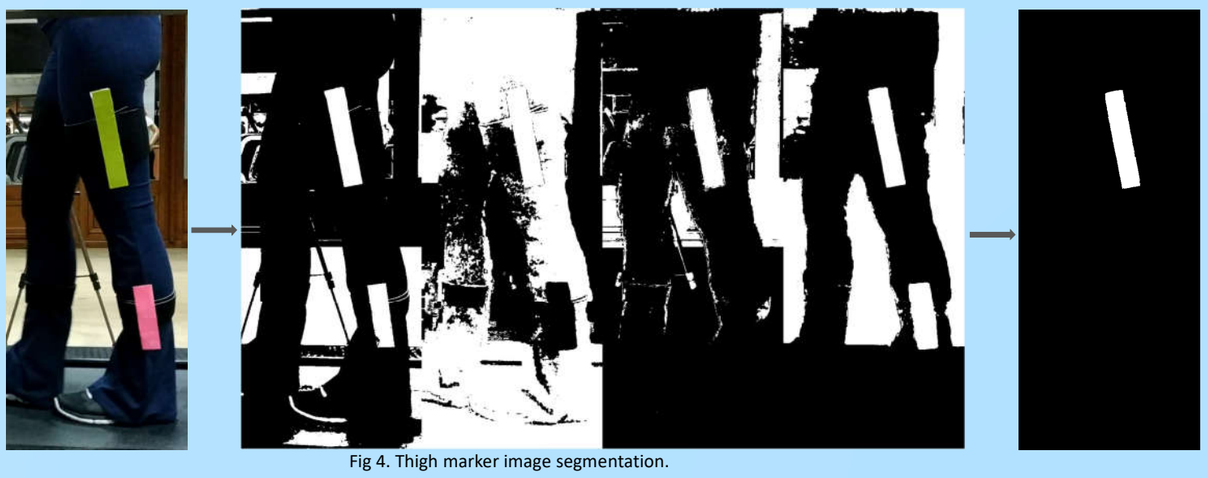

Fig 4. Thigh marker image segmentation.

Results

Table 1. RMSE parameter for each subject at the speed of 3 km/h.

Subject	*RMSE* [°]			
	Left thigh	Right thigh	Left shank	Right shank
ID1	2.9	1.54	1.97	3.67
ID2	2.64	2.27	2.12	4.11
ID3	1.43	1.3	2.78	4.13
ID4	1.13	2.78	2.56	4.47

Table 2. Maximal standard deviation of angle profiles for each subject at the speed of 3 km/h.

Subject	Maximal standard deviation: Mtw Awinda / Optical system[°]			
	Left thigh	Right thigh	Left shank	Right shank
ID1	2.44/2.89	2.04/2.07	3.24/3.55	4.22/4.89
ID2	2.46/2.11	2.60/1.89	2.64/2.55	2.63/2.21
ID3	1.86/1.83	1.78/1.87	3.75/3.70	2.31/2.81
ID4	1.42/1.54	1.39/1.63	2.36/2.59	2.17/2.56

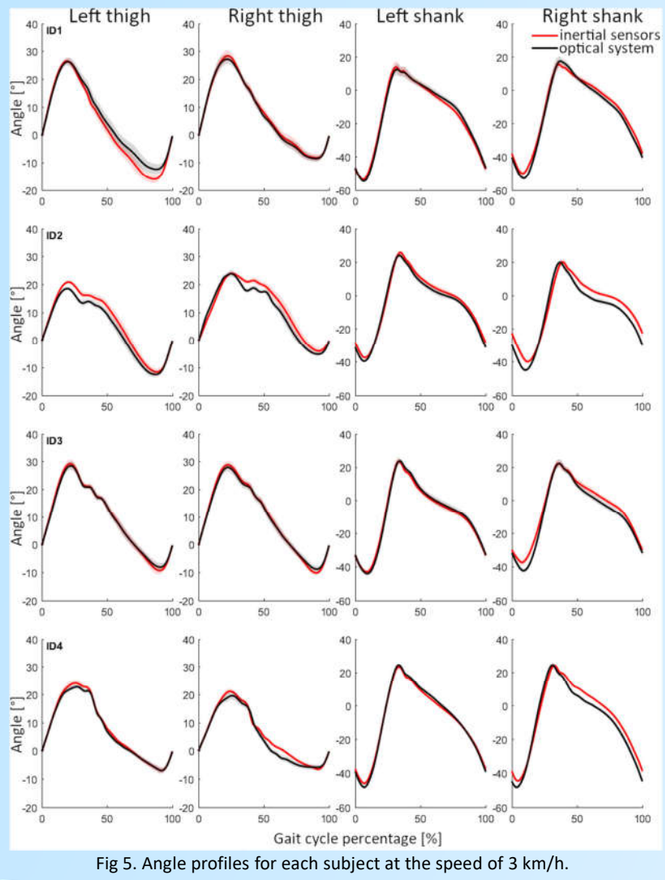

Fig 5. Angle profiles for each subject at the speed of 3 km/h.

Conclusion

The implemented optical system for gait analysis has shown good results in comparison to the reference system. Possible improvements of the system include cameras with higher framerate and lower exposure time in order to minimize the error coming from the blurriness of the markers in certain frames. A monochrome background or different types of markers could improve the precision of the system as well as remove possible false marker detection. For further upgrading of the system, more cameras and markers could be added in order to enable 3D motion tracking.

LABVIEW BASED CHESS CLOCK

Author: Petar Vidoevski

Faculty of Electrical Engineering & Information Technologies
Skopje

Abstract:
The goal of this project is to simulate the working principle of a chess clock using NI-DAQ 6008, LabVIEW and the model with controls and indicators that is used in the competition.

Key words: chess clock, data acquisition, LabVIEW

Introducton:
The working principle of the chess clock is the following. First the users pick the starting time (1,2,3,5,10,15,30,60 min) with clicking SW-1. After the picking of the of the starting time the users pick the increment (0,1,2,3,5,10,15,30,60 s). When the users are done with picking the increment they switch SW-3 and the game starts. For ending the turn player 1 uses SW-1 and player 2 uses SW-2 and after the finishing of the turn their time is incremented. The respective LED (1 or 2) are on when one of the players are making their move. When the players have less than 30 s left the LED starts to blink. The program ends when any of the players have no time left or the SW-3 is switched off.The chess clock indicator is off when player 1 and opposite for player 2.

Methodology:
The architecture used is state machine and it contains states for initializing default values, picking time and increment, state when the players are on the move, incrementing time and ending. The timer and picking of time and increment are done with functional global variables.Custom indicators are done for display and chess clock indicator.The data acquisition is done with DAQmx.

Front panel

Hardware

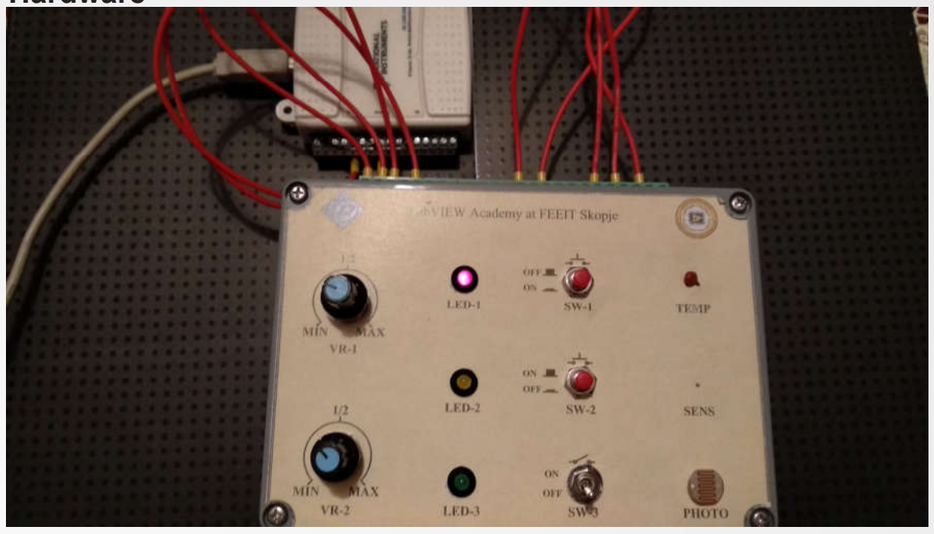

Initializing default values

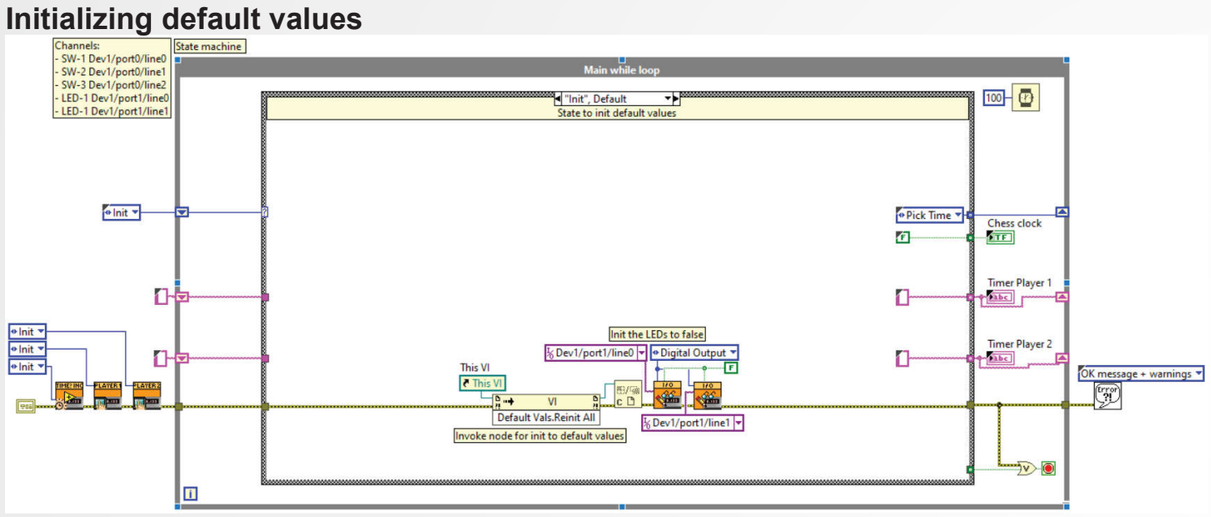

Picking time / increment

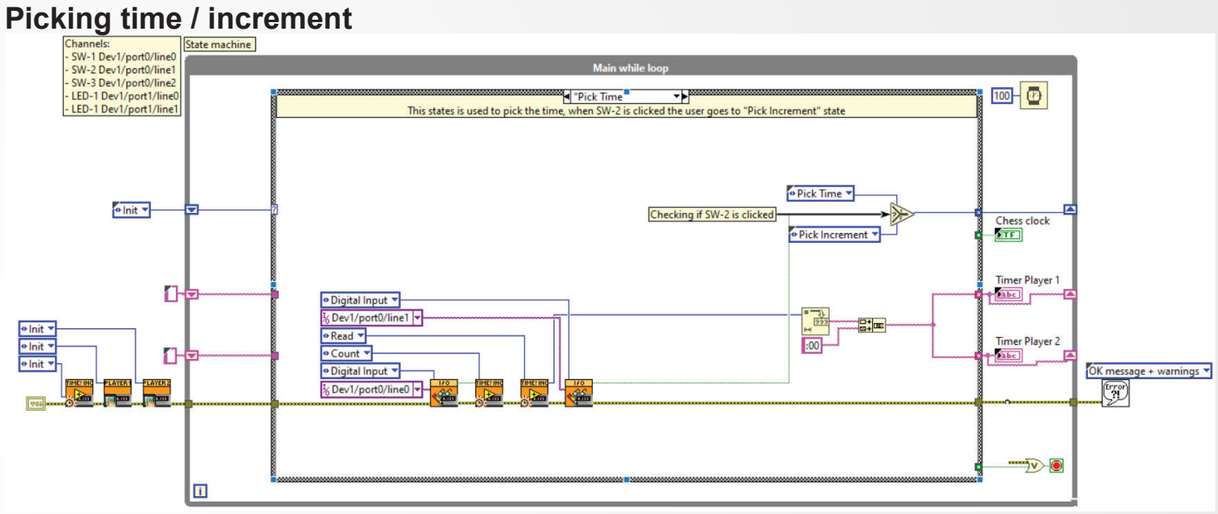

When is player's 1/2 turn

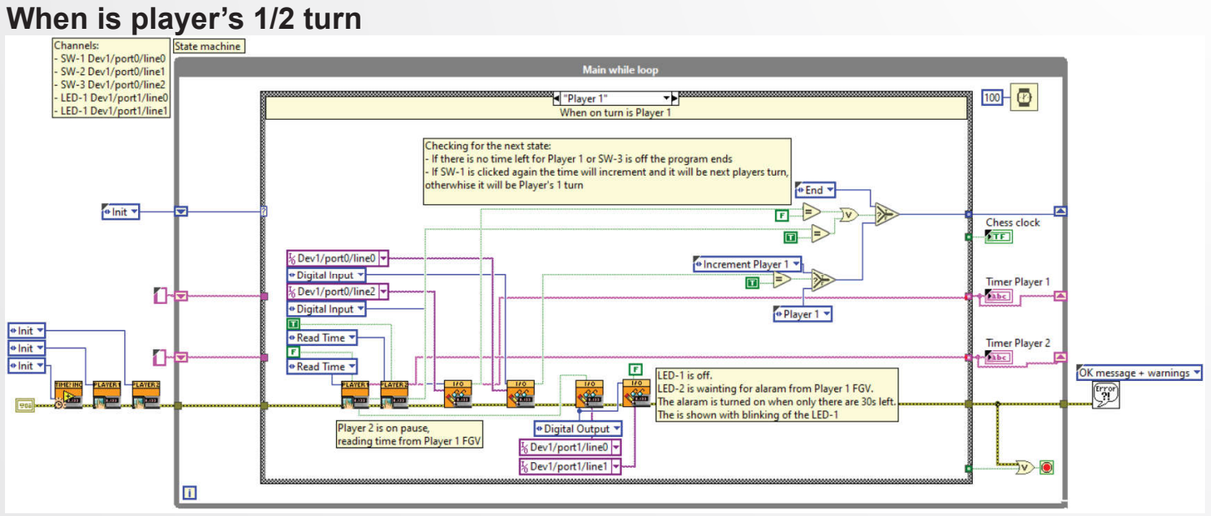

Incrementing time after finishing of the turn

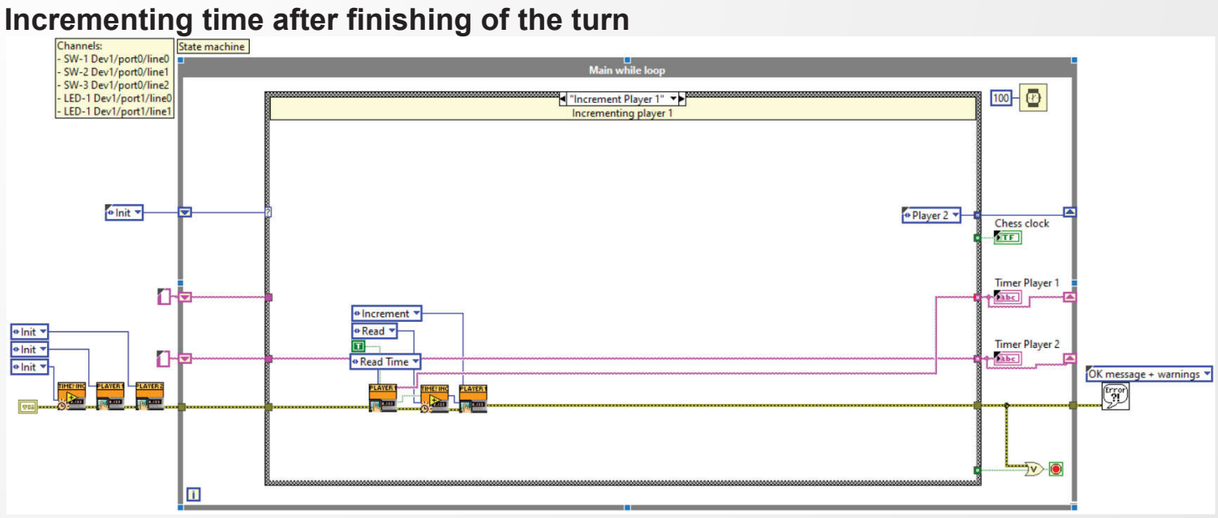

FGV for the reverse timer

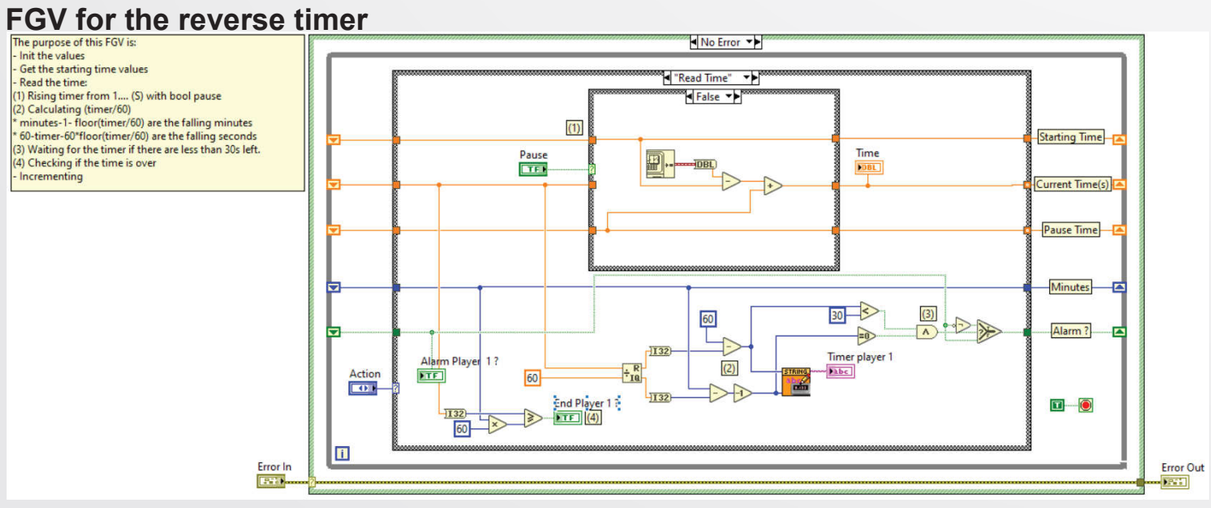

FGV that counts how much times Time or Increment is clicked

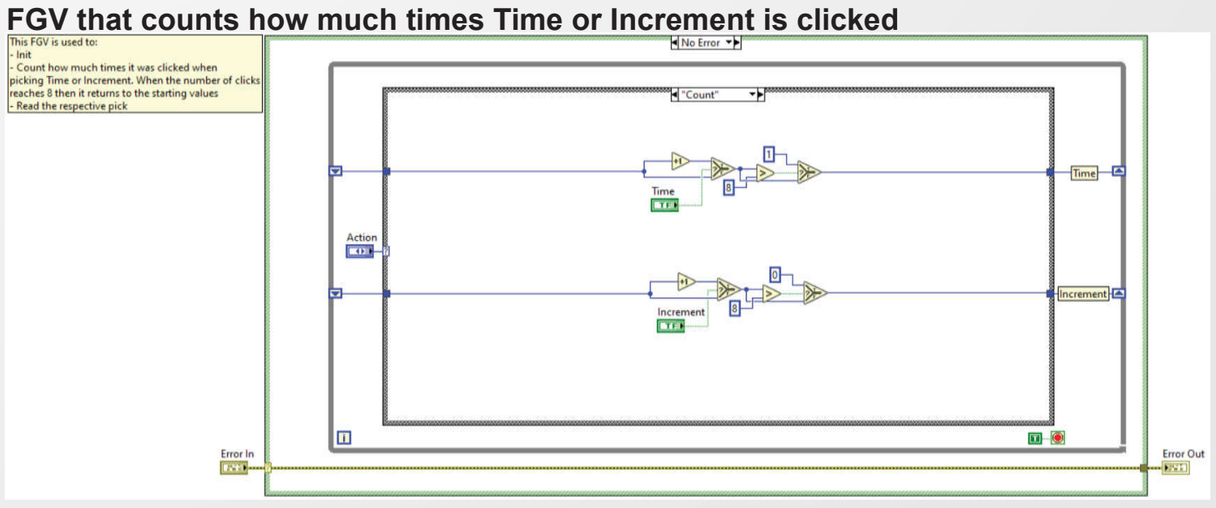

SubVI for digital input and output

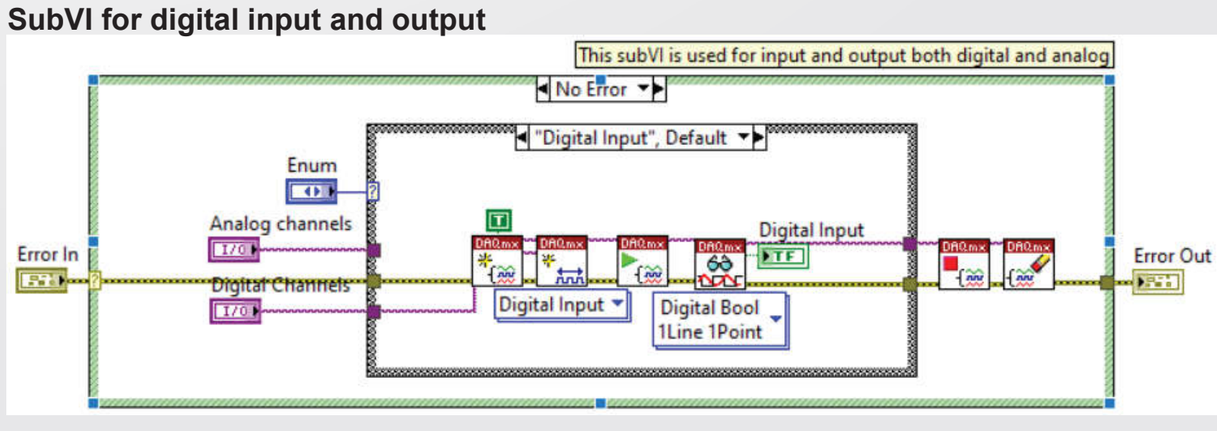

Conclusion:
This program can evolve to producer-consumer based chess clock

Acknowledgement:

I would like to thank my mentors Prof.Dr Zhivko Kokolanski and Bodan Velkovski for sharing their knowledge and contribution to the project.

Low-cost system for drowsiness detection

Ana Dodig, Nebojša Jovanović
University of Belgrade, School of Electrical Engineering

Abstract

The purpose of this paper is to demonstrate human physiological phenomenon of heart rate variability (HRV) and how it can be used to upgrade the existing driver drowsiness detection system. The aim of this system is to alert the driver when the signs of fatigue are detected using camera and heart rate sensor simultaneously. The software for video processing is written using OpenCV (Intel Corporation, Santa Clara, USA) computer vision library, and the algorithms for extraction of heart rate variability parameters are written in Python. The software operates on Raspberry Pi, which is small and relatively cheap computer. The results of this project can be used as an excellent platform for all drowsiness related topics, including building a low-cost and reliable driver drowsiness detection system.

Introduction

Why this topic is of interest to us?

- About 100,000 accidents per year are caused by drowsy drivers[1]
- The European Union is introducing a law that states that from 2022 year, all vehicles must have a drowsiness detection system[2]
- Therefore it is important to build a reliable, real-time, low-cost system
- Commercial systems are consisted of camera driver monitoring
- Can such a system be enhanced?
- Yes. By using physiological signals such as heart rate variability and analyzing its parameters such as LF/HF ratio. It was found that during the transition from wakeful to drowsy state, the heart rhythm decreases and that very low frequency (VLF) oscillations decrease, which predicts a change in the LF / HF ratio to parasympathetic dominance, thus, that ratio decreases[3].

Method

System description

Video is obtained from the web camera. For signal acquisition a Heart Rate sensor is used. The sensor reads the analog signal, which must be converted to digital using separate A / D converter, because the Raspberry Pi does not own the same. In FIG. 1 a diagram of the connected system is presented. One output pin of the Raspberry Pi is through a resistor connected to an LED that effectively serves as an alarm.

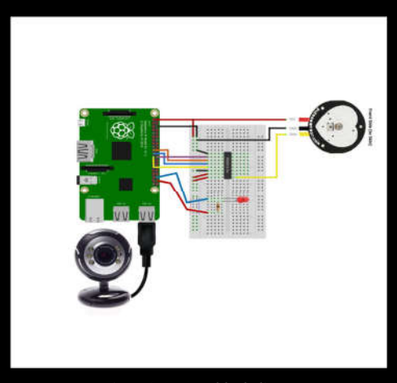

Figure 1. System block diagram

Camera

Camera is a method involving constant monitoring of the driver. In real time, the camera captures the driver, then the eye region is extracted. By analyzing the region obtained, it is possible to obtain information about whether the driver is closing eyes for a longer time, which would suggest that the driver is drowsy. If the camera detects that the eyes have been closed for more than 0.3 seconds, an alarm goes off. In this way, eye blinks are not detected because the average human blink lasts between 0.1 and 0.15 seconds. EAR (Eye aspect ratio) is the value that we measure and is calculated as: $EAR = \frac{\|p_2 - p_6\| + \|p_3 - p_5\|}{2\|p_1 - p_4\|}$ (fig. 6) [4].

Respondent ID	Age	Gender	Height [cm]	Weight
ID1	21	Male	185	83
ID2	19	Male	186	79
ID3	52	Female	170	80
ID4	52	Male	175	90

Table 1. List of respondents

HRV (Experiment description)

Two experiments were performed. The first experiment was done before signal acquisition and processing, a series of offline recordings were conducted to train a classifiers based on training set. Recording time is 250 seconds. The description of the respondents is given in Table 1. The obtained results were used as a vector of predictors for the calculation of classification parameters. The classifier used is binary logical regression. In order to validate the system, 30 LF/HF values were measured in the second experiment, 15 during the day and 15 during the night. As measurements were made in real time, it was necessary to have a "warm-up" time during which data were collected. The first LF/HF value is determined after 120 seconds and the next ones were obtained every 30 seconds. This value is then passed to the classifier, which outputs 0 - not drowsy or 1 - drowsy after which the alarm goes off, in our case an LED connected to a circuit with a Raspberry Pi computer [5].

Results

Figures 4 and 5 show the spectrograms of the awake and sleepy subjects. As it can be observed drowsy subjects have a higher proportion of power at higher frequencies, which effectively reduces the LF / HF ratio, as theoretical predictions suggest.

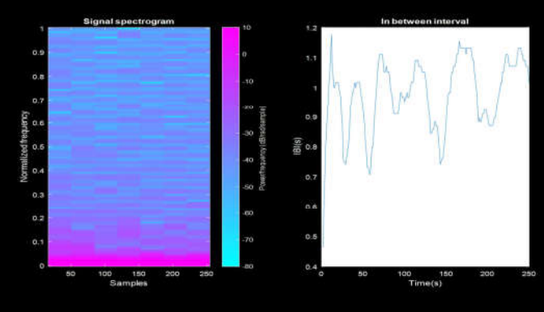

Figure 4. Spectrogram of an awake subject

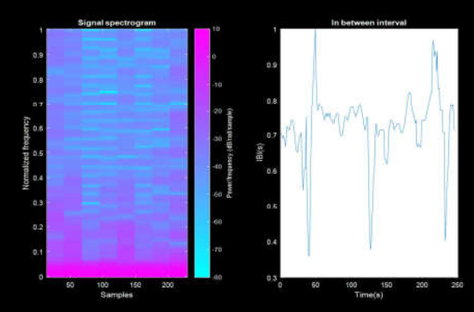

Figure 5. Spectrogram of a drowsy subject

The real-time EAR is shown in Fig. 6. A sudden drop in value occurs when subject blinks. The EAR threshold for blink detection is 0.2

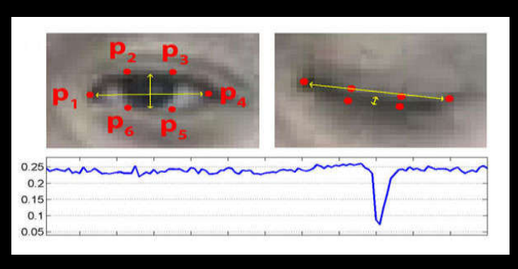

Figure 6. EAR values in real time

After the second experiment the following results were obtained which are given in Table 2.

True negative	False negative	True positive	False positive
15	2	11	2

Table 2. Number of correct and incorrectly detected LFHF ratios

Based on these results, the characteristics of the system can be determined:
specificity = 0.882, **sensitivity** = 0.846, **precision** = 0.846, **accuracy** = 0.867

Discussion & Conclusion

The power of spectral components at low (0.04 Hz to 0.15 Hz) and high (0.15 Hz to 0.4 Hz) frequencies are analyzed in this paper. This ratio is referred to as LF / HF, where LF reflects a measure of sympathetic activity and HF a measure of parasympathetic activity.
Based on the obtained results, it is concluded that a relatively simple and inexpensive prototype of the system has been developed.
Some improvements can be made:

- Application of machine learning and AI in the analysis of LF/HF ratio
- Better quality hardware components, most notably Heart rate sensor
- The system can be implemented in any motor vehicle with a few adjustments. An electrical power system needs to be built so that the power of the computer processing the signals is adjusted to the battery voltage of the vehicle

Other options for realizing the alarm are possible through the sound signal or the vibration in the steering wheel.

Acknowledgement

The authors thank the Laboratory for Biomedical Engineering and Technologies, Department of Signals and Systems, Faculty of Electrical Engineering in Belgrade for funding this project and the opportunity to use the laboratory, and especially Doc. dr. Milica Jankovic as a mentor and on suggestions for writing the paper.

Contact

Ana Dodig, Nebojša Jovanović
University of Belgrade, School of Electrical Engineering
Email: ana.dodig97@gmail.com, nebojsa.php@gmail.com

References

1. National Highway Traffic Safety Administration
2. European Commission – Press release, Brussels, 26 March 2019
3. TASK FORCE OF ESC AND NASPE. Heart rate variability: Standards of measurement, physiological interpretation, and clinical use. Circulation 1996; pp. 1043-1065
4. Tereza Soukupova and Jan Čech, *Real-Time Eye Blink Detection using Facial Landmarks* 2016.
5. A.J. Camm *et al.,* "Guidelines heart rate variability – standards of measurement, physiological interpretation, and clinical use," *Eur. Heart J.,* vol.115, no.5, pp. 354-381, 1996.

LabView based platform for control and monitoring of a six-phase electrical drive

Strahinja Aškrabić

School of Electrical Engineering, University of Belgrade

Abstract

A LabView based platform for control and monitoring of a six-phase electrical drive is developed in the Laboratory for Electrical drives at the School of Electrical Engineering in Belgrade. Three-phase and six-phase scalar control algorithms have been implemented for demonstration purposes. The software base of the platform is a program developed in National Instruments LabView programming language.

Introduction

One of the main tasks of modern society is to introduce new, flexible and efficient electrical drives. Previous research has shown that five or six-phase drives have greater efficiency, reliability and better performance than three-phase drives, which is especially important in high power applications. Of course, application of six-phase induction motors requires adequate power converters and control algorithms.

Metodology

Main components of the platform are two three-phase **"SEMIKRON SEMITEACH IGBT"** power converters, **"Power Electronic & Drives Board-PED Board"** control unit, two boards for measurement of three phase currents each equipped with **"LEM"** current sensors and **"HVSB"** voltage sensor board for per-phase and DC voltage measurement. The platform is modular and very flexible, so it can be easily upgraded with other sensors and devices (e.g. encoders or resolvers).

"SEMIKRON SEMITEACH IGBT" power converters are 20kW three-phase ac/dc/ac converters with a maximum of 20 kHz switching frequency. This devices are developed for educational and laboratory purposes, so all their components are well-designated and can be easily distinguished, which is very important for students. At their input is a three-phase diode bridge rectifier. The output stage is a three-phase voltage inverter with powerful **IGBT** transistors. The DC link with 0.88-1.32 mF capacitors and a braking chopper and an optional braking resistor are connected between the input and the output.

"Power Electronic & Drives Board-PED Board" control unit is equipped digital and analog inputs and outputs. This control unit contains an FPGA chip and it is programmable via **NI LabView** programming language. Use of LabView represents a major advantage, because it allows implementation of complicated real-time control or optimization algorithms which can be executed at high sampling rates thanks to the **FPGA** chip. Apart form the implementation of the control algorithms, LabView also allows development of an interactive user interface. This powerful software enables the user to control and supervise the drive and to aquire important data.

The monitoring system allows the user can monitor four phase currents and two phase voltages which are directly measured by the sensors. User can also monitor calculated values as dq an xy components and complex components of the current values. Data can be exported to an Excel spreadsheet for storage and further analysis.

Soft start with adjustable ramp-up time of the frequency reference is realized as part of the control algorithm. For the three-phase algorithm, U/f control is applied. U/f is realized as aproximate piecewise linear relationship that can be adjusted by user. For six-phase control, the user specifies *Udq* and *Uxy* voltage components, and the phase angle *fixy*, so voltage references are calculated as:

ua1xy = Uxy*cos(ωt + fixy)	ua1dq = Udq*cos(ωt)
ub1xy = Uxy*cos(ωt – 4π/3 + fixy)	ub1dq = Udq*cos(ωt – 2π/3)
uc1xy = Uxy*cos(ωt – 8π/3 + fixy)	uc1dq = Udq*cos(ωt – 4π/3)
ua2xy = Uxy*cos(ωt – 5π/6 + fixy)	ua2dq = Udq*cos(ωt – π/6)
ub2xy = Uxy*cos(ωt – π/6 + fixy)	ub2dq = Udq*cos(ωt – 5π/6)
uc2xy = Uxy*cos(ωt – 3π/2 + fixy)	uc2dq = Udq*cos(ωt – 3π/2)
Phase voltages:	
ua1 = ua1dq + ua1xy	ua2 = ua2dq + ua2xy
ub1 = ub1dq + ub1xy	ub2 = ub2dq + ub2xy
uc1 = uc1dq + uc1xy	uc2 = uc2dq + uc2xy

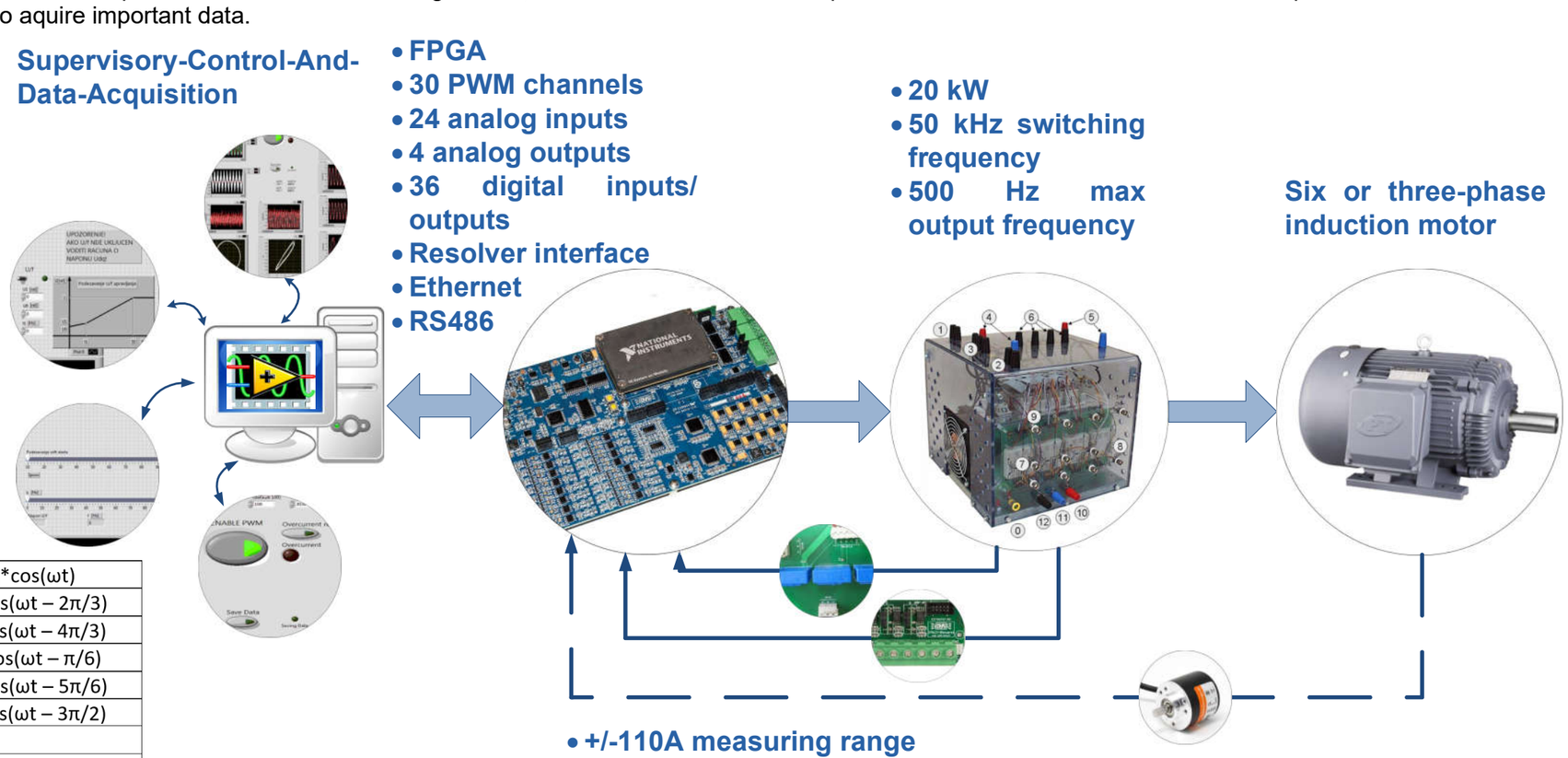

The control algorithm is separated in two parts. One part of the algorithm, that requires high rate execution (PWM, inputs sampling...) is realized as FPGA code. The other part, (setting the voltage and frequency reference, current and voltage monitoring) that does not require such high execution rates, is implemented in the processor. Even though the power converters have their own protections, additional software overcurrent protection is implemented as a part of the algorithm. For measurement purposes, analog inputs of "Power Electronic & Drives Board-PED Board" control unit are equiped with second order low-pass Butterworth filters.

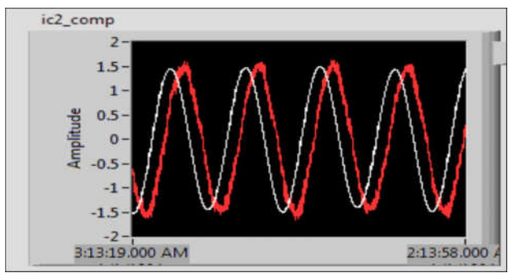

Measured Phase current

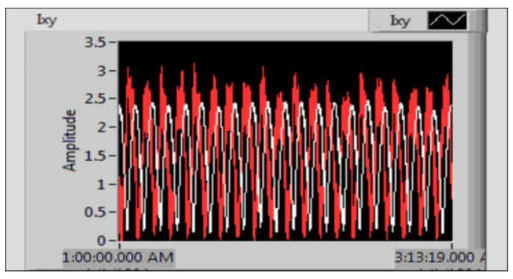

Calculated xy component of currents

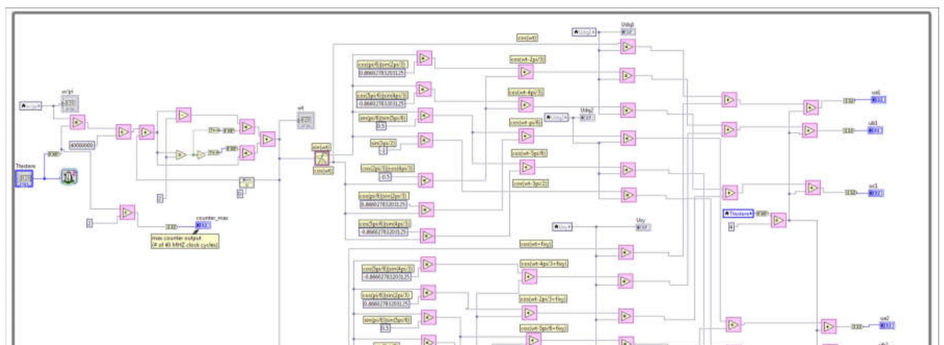
Calculating of six-phase reference voltages on FPGA in fixed point aritmetics

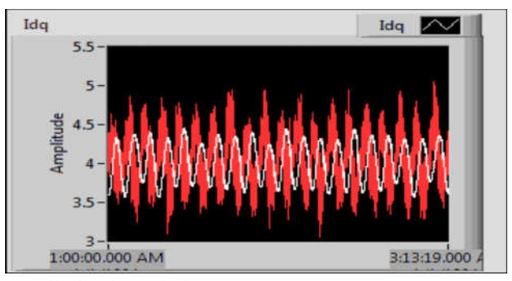

Calculated dq component of currents

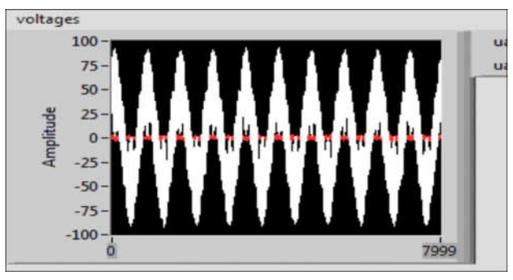

Measured voltages

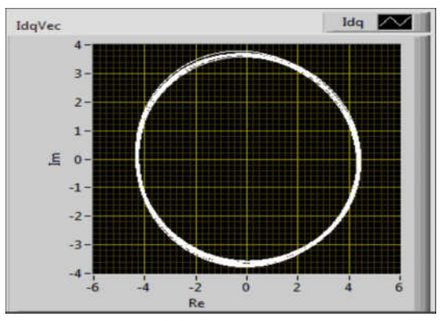

Idq vector

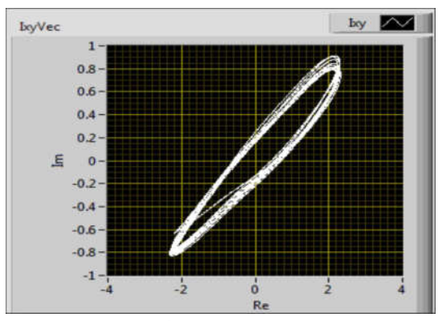

Ixy vector

Conclusion

The developed platform has proven to be a very reliable and user-friendly solution for the control of a six-phase electrical drive. The result is a very modern laboratory electrical drive control and monitoring system with a great educational and research potential. Students and researches can use the setup for testing and developing of modern control algorithms which are necessary as part of the sustainable power industry.

Acknowledgement

I would like to express my sincere gratitude to my supervisors Dr. Leposava Ristić, Dr. Milan Bebić and Msc. Bogran Brković for providing their invaluable guidance, comments and suggestions throughout the course of the project.

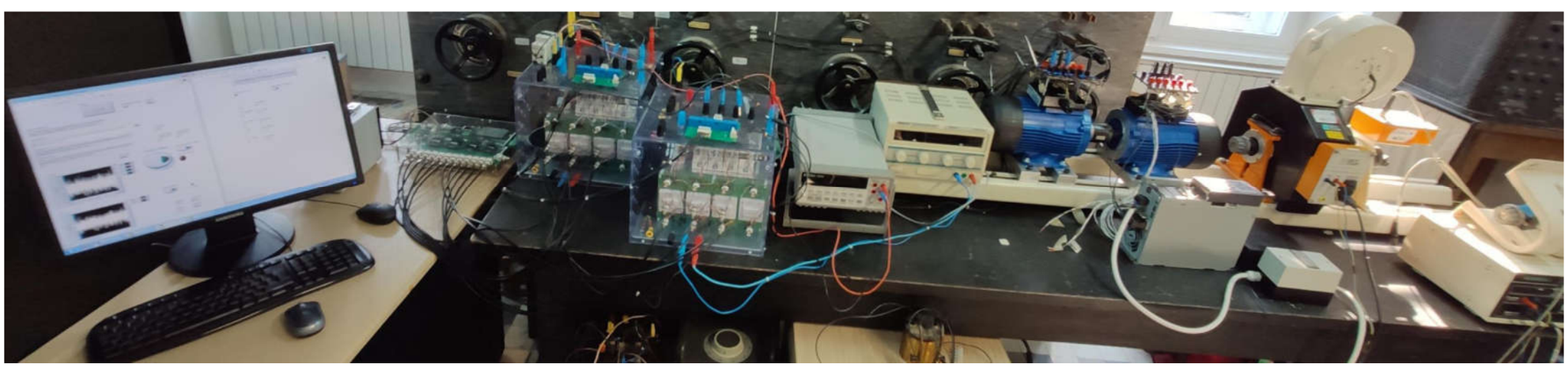
LabView based platform for control and monitoring of a six-phase electrical drive

Experimental Identification of Dynamic Parameters for Industrial Robots

Author: Marija Bogosavljević

School of Electrical Engineering, University of Belgrade, Serbia

ETF Robotics

DILLON

Resume

This paper focuses on determining the set of dynamic parameters of a six-axis **Denso VP-6242** industrial robot. Identification is performed by the **experimental method** [1], which implies that the parameters of a dynamic model are estimated using the data contained in the robot's response and measured during a specially designed experiment. First, a symbolic set of dynamic parameters must be determined, based on the **DH parameters** of the industrial robot [2], and then model identification is performed by solving the Inverse Dynamic Identification Method (IDIM). After that, the obtained parameters of the dynamic model are **optimized** by the least-squares method. The final identification step is **model validation**, based on the comparison of measured and estimated torque. This model represents the dynamic relationship between the joint torques and joint positions.

The IDIM equation, or the **motion equation** according to the Lagrange or Newton-Euler formalism [3] is:

$$M(q)\ddot{q} + C(q,\dot{q})\dot{q} + g(q) = \tau. \quad (1)$$

For an industrial robot with n segments, τ is the n-vector of actuator torques as well as the joint positions q, velocities $\dot{q}$, and accelerations $\ddot{q}$. $M(q)$ is the $n \times n$ symmetric and positive definite inertia matrix, $C(q,\dot{q})$ denotes the n-vector of Coriolis and centrifugal forces, and g is the n-dimensional vector of gravitational forces [4].

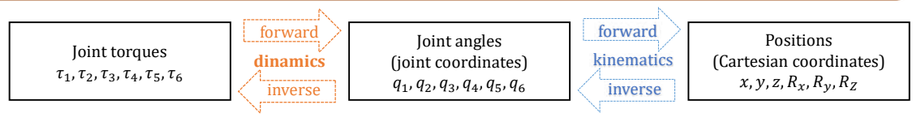

The simplification of the motion equation in the linear form [5] is:

$$\tau = H(q,\dot{q},\ddot{q})\delta, \quad (2)$$

where H is $n \times n_\delta$ observation matrix, and δ is n_δ-vector of dynamic parameters. In general, not all the dynamic parameters have the same influence on the model, and only the minimum-set of dynamic parameters, so-called **base parameters**, can be identified. Consequently, the IDIM based on basic dynamic parameters can be rewritten as

$$\tau_C = H_B(q,\dot{q},\ddot{q})\beta\,, \quad (3)$$

where β is n_β-vector of base parameters, and $n_\beta < n_\delta$. The result of experimental procedure is a set od estimated robot dynamics parameters $\hat{\beta}$.

Introduction

For the experiment purposes, it is necessary to achieve *master-slave* communication between the robot controller and the computer. Designing an experiment requires knowing the limitations of the robot:

- working range of the robot - workspace
- maximum load weight
- maximum joint speeds
- maximum joint torques

In this paper, the robot has no payload on its end-effector while performing the experiment.

A dynamic manipulator model is required for advanced Model-Based Control (MBC) algorithms or Kalman filter formulations when designing adaptive algorithms. When there is another robot or human in the environment of the robot, and there is a Physical Human-Robot Interaction (PHRI) between them, the implementation of protective collision detection techniques is necessary, i.e. collision with the robot environment requires knowledge of robot's dynamics.

Dynamic model is affected by physical components such as motors, gearboxes, etc. - they are constantly consumed and their characteristics change.

Robot's dynamic model changes over time ⇨ Algorithms cease to be optimal over time ⇨ **The dynamic parameters model needs to be updated!**

Methodology

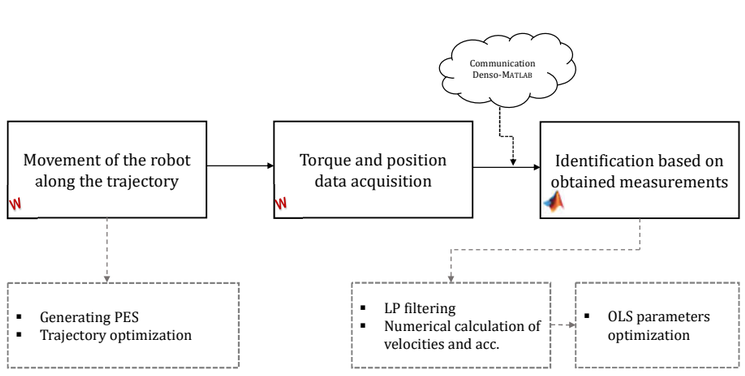

Dynamic parameter identification can be divided into sections that include:

- Specification of robot trajectory in the **Wincaps** software tool for Denso robot programming:
  - movements are specified individually for all joints, taking into account the minimum and maximum angles which can be realized by a certain joint [6] (Figure 1)
  - in this work the trajectory is given by the *ad-hoc* method, that is, manually pointing the robot to points inside the workspace; the robot repeats the trajectory while data is being collected
- Signal processing in the **MATLAB** software tool, which includes:
  - calculating velocities and accelerations based on the measured joint position data (Figure 2)
  - processing of the obtained torque data achieved during the movement of the robot along the given trajectory
  - filtering the measured data with a low-pass Butterworth filter (Figure 3)
  - parameters optimization by the ordinary least-squares method
  - model validation based on the comparison of measured and estimated torque (Figure 4)

Prior to parameter identification itself, a symbolic vector of base parameters is obtained using the **SymPyBotics** software tool.

Only the results of the first, third and fifth joint are shown.

1. Excitation trajectory

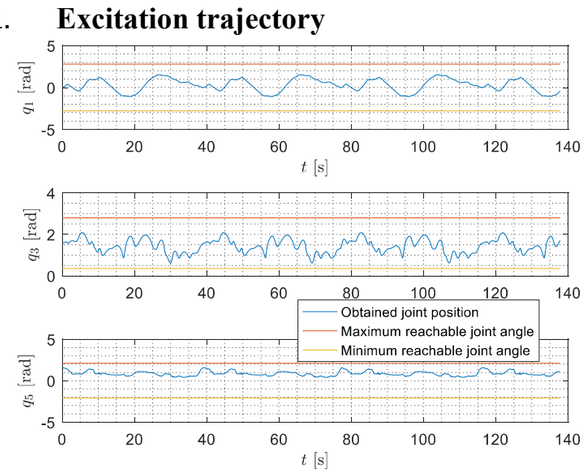

2. Joint velocity and acceleration estimates

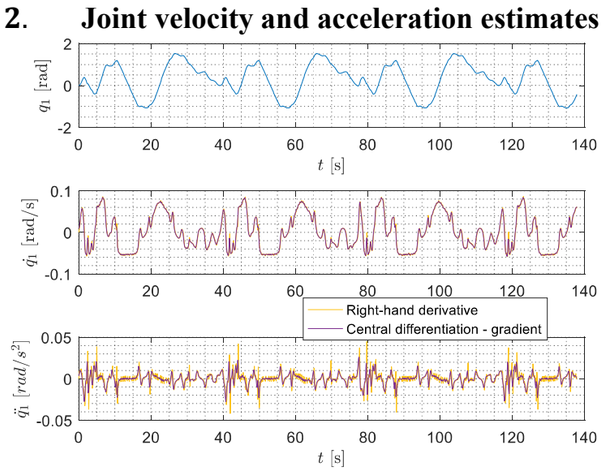

3. Signal filtering

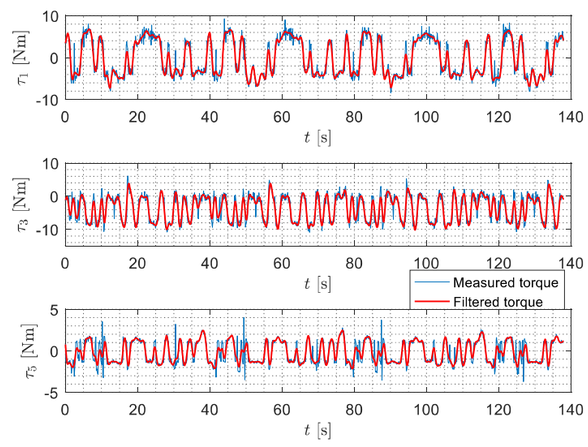

4. Model validation

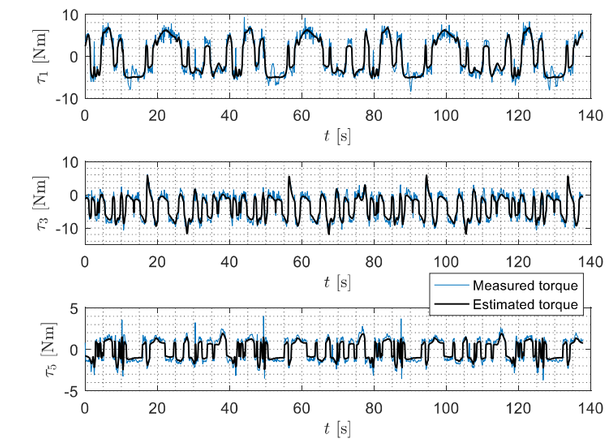

Conclusion

The proposed identification method identified 31 of 48 base parameters and a total of 72 dynamic parameters for Denso VP-6242 industrial robot. To achieve better results, a few changes need to be done:

- Trajectory optimization according to robot constraints instead of *ad-hoc* method
- More adequate filtering, i.e. signal processing
- Use of MDH instead of DH because it affects the set of base parameters [6]
- Parameter optimization based on the physical sense of the parameters (to avoid impossible parameter values)
- Combining different measurements (moments and currents) to identify more parameters [7]

The resulting set of dynamic parameters is validated based on the comparison of measured and estimated torque. Torque estimation can be further used in the design of advanced control algorithms, and one of the techniques is Computed Torque Control – CTC.

To be able to update the dynamic model in real-time, it is necessary to create an algorithm that will estimate at which point the deviation of the dynamic parameters occurred. Depending on the application of the robot, the work assignment can potentially be used as an excitatory signal for the experiment.

References

[1] Walter E., Prozanto L., (1997). „Identification of Parametric Models from Experimental Data". Communications and Control Engineering. Springer-Verlag London, 1st edition.
[2] Denavit J., Hartenberg R. S. (1955). *A kinematic notation for lower-pair mechanisms based on matrices*, Journal of Applied Mechanics 1.
[3] Borovac B., Đorđević G., Raković M., Rašić M., (2017). „Industrijska robotika", FTN izdavaštvo, Novi Sad.
[4] Vuong N.D., Marcelo H. Ang Jr. (2009). *Dynamic Model Identification for Industrial Robots.* Article in Acta Polytehnica Hungarica.
[5] Swevers J., Verdonck W., Schutter, J. (2007). *Dynamic Model Identification for Industrial Robots*. IEEE Control Systems Magazine.
[6] Bahloul A., Tliba S., Chitour Y. (2018), *Dynamic Parameters Identification of an Industrial Robot With and Without Payload*. IFAC. 18th IFAC Symposium on System Identification, SYSID 2018, Stochkolm, Sweden.
[7] Jubien A., Gautier M., Janot A. (2014). *Dynamic identification of the Kuka LWR robot using motor torques and joint torques sensor data.* Proc.of the 19th World Congress, The IFAC, Cape Town, South Africa.

Acknowledgment

The experimental phase of this project was supported by Dillon Robotics Ltd., Belgrade. http://dillonrobotics.com/eng/

Antagonistic Tendon Driven VSA Control Through the Matlab/Simulink and LabVIEW Integration

Milan Knežević, University of Belgrade – School of Electrical Engineering

The focus of this paper is an implementation platform for quickly and simple analyzing of a control algorithm for robotics joint with variable stiffness. The main goal is achieving a possibility to test control algorithms, written in the Matbal&Simulink programming environment, directly on the real system. The cascade control algorithm described in [1] is divided into two executing parts. First part represents a lower control loop, loop for controlling actuators, executing on FPGA chip. FPGA chip, due to its speed and determinism which cannot be achieved by another system like PC, represent the perfect choice for executing a fast lower control algorithm. The second part represents a higher control loop, loop for controlling nonlinear multivariable systems, like controlling position and stiffness of antagonistic robot joint, executing on PC using Matlab&Simulink program. Choosing Matlab&Simulink for higher control loop gives flexibility for solving the problem of controlling the antagonistic robot joint. In addition to PC (Matlab&Simulink) and FPGA chip, system contain also Real-Time controller used as a communication and control mechanism between these two executing platforms.

In the growing fields of wearable robotics, rehabilitation robotics, prosthetics, and walking robots, variable stiffness actuators (VSAs) or adjustable compliant actuators are being designed and implemented because of their ability to minimize large forces due to shocks, to safely interact with the user, and their ability to store and release energy in passive elastic elements[2]. A compliant actuator will allow deviations from its own equilibrium position, depending on the applied external force. The equilibrium position of a compliant actuator is defined as the position of the actuator where the actuator generates zero force or zero torque. This concept is specifically introduced for compliant actuators, since it does not exist for stiff actuators. Passive compliant actuators contain an elastic element, i.e., a spring that can store energy—which is not the case for actuators with active compliance, where the controller of a stiff actuator mimics the behavior of a spring.

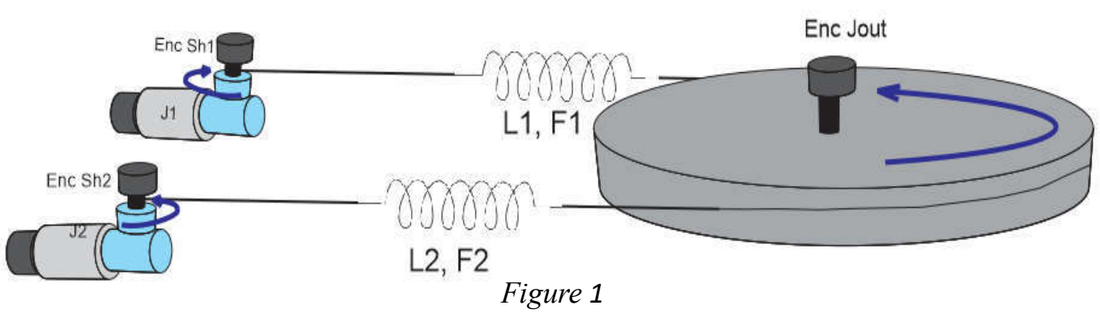

Figure 1

- **Biological Inspired Joint Stiffness Control**

This biologically inspired joint stiffness control is a rotational joint, actuated by two SEAs as shown in Figure 1. When both servomotors rotate in the same direction, the equilibrium position of the joint is changed. When they rotate in the opposite direction, the stiffness of the joint will be changed. It is important to mantioned that the nonlinearity of the spring is essential to obtain the adaptable compliance[3].

Controlling HW contains cRIO controller from National Instruments with appropriate modules for motor control and measuring analog inputs. System components:

- **NI cRIO 9074 [5] –** Real-Time embedded controller with FPGA ship
- **NI 9505 [6] –** module for controlling actuators
- **NI 9205 [7] –** module for measuring analog voltage signals

Software implementation is divided into four independent application which communicates with each other through different and predefined protocols.·

- **Matlab&Simulink plugin** – supporting code for communication between PC and controlling system
- **Real-Time application** – application for controlling FPGA execution and provide communication between PC and FPGA
- **FPGA control and measure application** – FPGA implementation of controlling algorithms and measuring system signals
- **LabVIEW configuration and monitoring application** – application for connection configuration between PC and FPGA and monitoring of system signals measured by FPGA application

Figure 3 shown communication protocols used in communiication between applications.

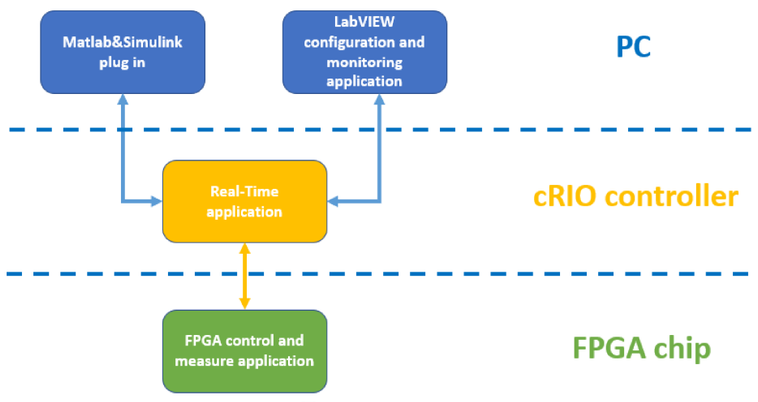

Figure 2

Communication is done by two protocols:

- **TCP/IP –** communication between configuration and monitoring application and Real-Time application.
- **UDP – c**ommunication between *Matlab&Simulink* Real-Time application

In addition to this protocol's application used build in communication between FPGA chip for exchanging data between Real-Team application and FPGA chip.

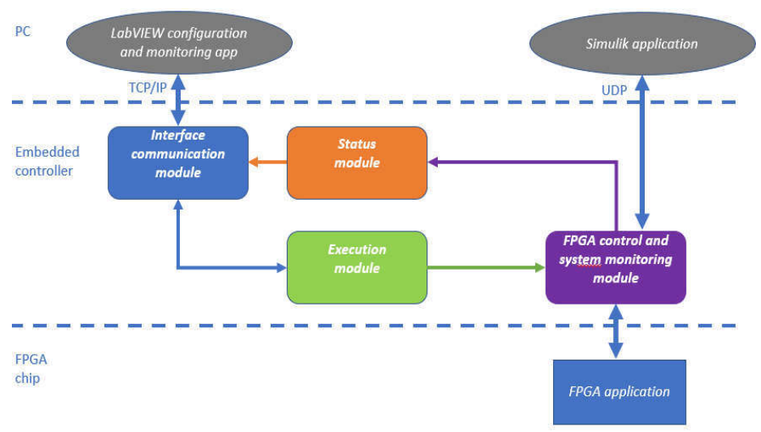

Figure 3

Lower control loop, motor controlling algorithm, contains three PIDs connected in cascade. Through the configuration tool user can configure the final lower control algorithm by enabling/disabling and defining PID parameters for each of these three PIDs. Structure of motor control algorithm implemented in FPGA:

- **Speed controller**
- **Position controller**
- **Current controlle**r

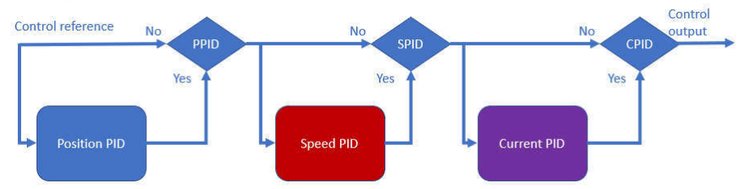

Figure 4

In this paper, it is shown the implementation of the cascade control algorithm. Higher and lower control loop are implemented in Matlab&Simulink and FPGA chip, respectively. This implementation brings two main advantages. Lower control loop implemented in FPGA chip gives higher performance compared to the same control loop implemented on PC or Real-Time controller. Higher control loop implemented in Matlab&SImululink brings freedom for choosing approach in solving nonlinear multivariable systems that can be applied to control position and stiffens of antagonistic robot joint.

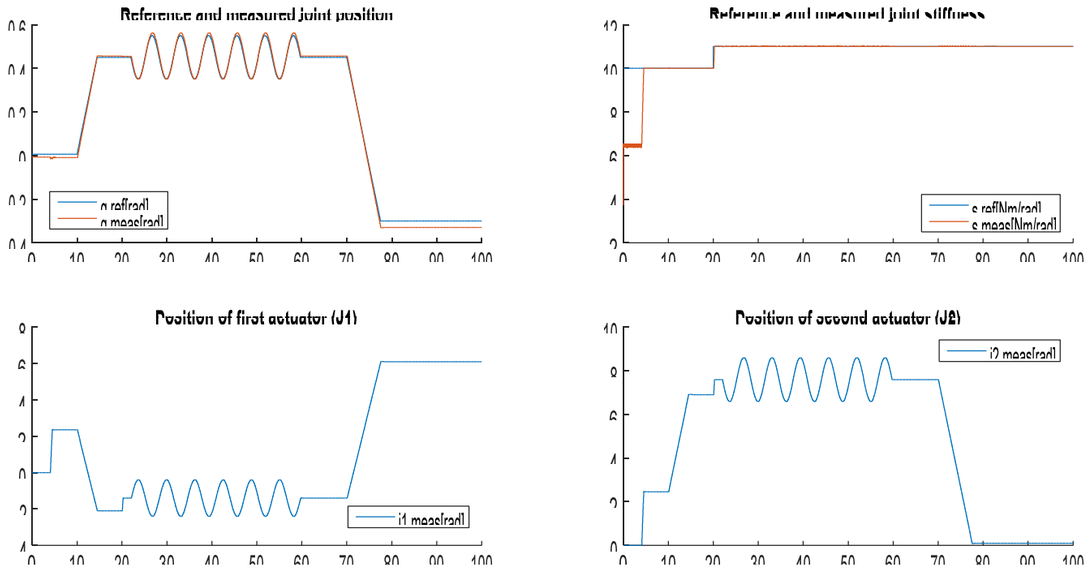

Figure 5

Implemented platform brings possibility to test and run cascade algorithms on real hardware without knowledge of LabVIEW programming language and system implementation in detail.

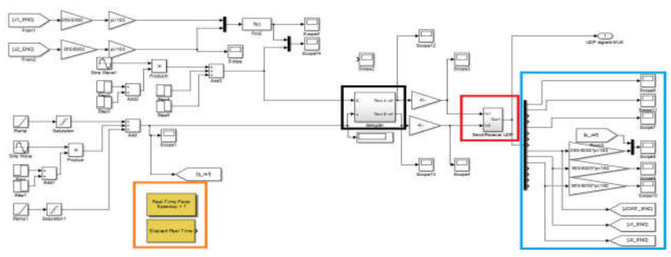

Figure 6

For video with platform in action please scan QR code:

Literature

1. Lukić, Branko & Jovanovic, Kosta & Šekara, Tomislav. (2019). Cascade Gain Scheduling Control of Antagonistic Actuators Based on System Identification: Proceedings of the 27th International Conference on Robotics in Alpe-Adria Danube Region (RAAD 2018). 10.1007/978-3-030-00232-9_45.
2. R. V. Ham, T. G. Sugar, B. Vanderborght, K. W. Hollander and D. Lefeber, "Compliant actuator designs," in *IEEE Robotics & Automation Magazine*, vol. 16, no. 3, pp. 81-94, September 2009. doi: 10.1109/MRA.2009.933629
3. S. A. Migliore, E. A. Brown and S. P. DeWeerth, "Biologically Inspired Joint Stiffness Control," *Proceedings of the 2005 IEEE International Conference on Robotics and Automation*, Barcelona, Spain, 2005,pp. 4508-4513. doi:10.1109/ROBOT.2005.1570814
4. https://www.ni.com/en-rs/support/model.crio-9074.html
5. http://www.ni.com/pdf/manuals/374211h.pdf
6. http://www.sal.wisc.edu/PFIS/docs/rss-nir/archive/public/Product%20Manuals/ni/ni-9205-manual.pdf

Image based method for assessment of water holding capacity of a meat sample

Miloš Lazić
University of Belgrade, School of Electrical Engineering

INTRODUCTION

Meat quality testing is carried out in order to decide on the usability of meat for human consumption. Water holding capacity is the ability of meat to retain its own or added water and is a characteristic of the quality of meat on the basis of which meat is classified for the production of particular meat products. Water in muscles can be bound in two ways: by chemical bonds or by physical forces. Chemically bound water and water immobilized in capillary structures are lagging behind.

The water that meat can release is called free water. There are several methods for estimating the water holding capacity of a meat sample, the most common methods being based on the application of force to squeeze free water and measure its quantity.

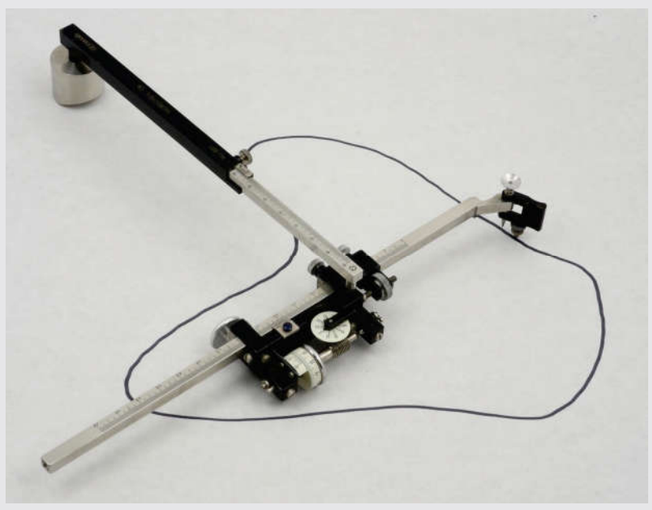

Figure 1. Planimeter

The parameter of water-holding capacity is most often determined by the planimeter compression method which is well represented in the professional literature. The meat sample by compression leaves a mark on the filter paper and the surface of the squeezed juice is measured by a planimeter. Unfortunately, the method takes a long time and requires the skill of the evaluator. It can also result in high measurement error which influences the decision on further production.

In this poster presentation, we propose a solution that is accurate, gives fast results, and does not require operator training. The aim of our research was to develop a simple and robust method for determining the water holding capacity of meat. The proposed method is based on the algorithms used in digital image processing.

METHODS AND RESULTS

The algorithm for calculating the displaced water is based on segmentation with further image processing for Binary object analysis. The measurement procedure is consisted of the following steps:

1. Place the meat sample on the filter paper and put it in the compressorium.
2. Wait for five minutes in order for the meat to release all of the water.
3. Place the compressorium on the stand and take a picture of the samples.

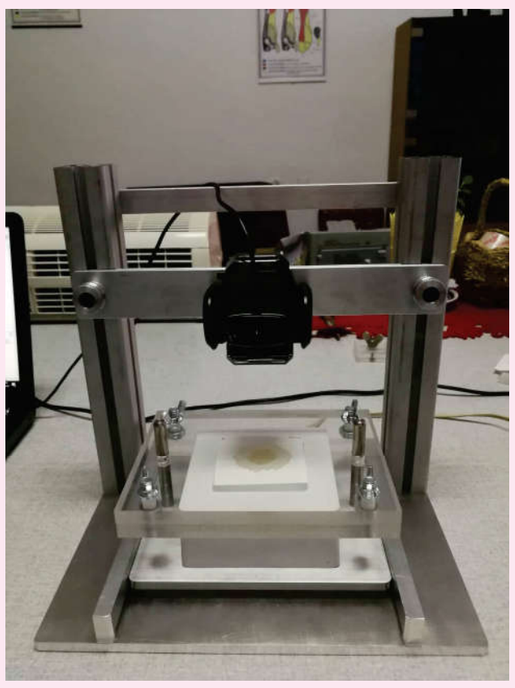

Figure 2. Acquisition system with a positioned meat sample

4. Insert a sample image into the program.

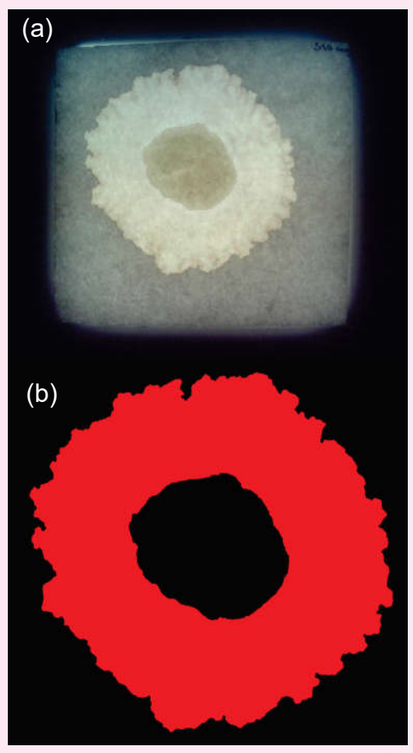

Figure 3. (a) The original image obtained from a web camera, and (b) the binary region obtained by the algorithm

5. Read the value obtained in the program.

By processing and segmenting the image, we have successfully separated the region that represents the displaced water from the meat sample. Now with simple operations on a binary image we can count the pixels and get the value of the required area.

Since we have the value of the surface expressed in cm², by multiplying by 10 we get the value of free water in mg. The multiplication factor is 10 because a 1cm² filter paper absorbs 10 mg of water. The algorithm is implemented in the “National Instruments - Vision Assistant 2019” software package. We used a standard general purpose web camera.

Table 1. Comparison of values obtained by planimeter and our algorithm

Sample	Planimeter [cm²]	Algorithm [cm²]
1	16,01	14,58
2	10,92	10,38
3	8,95	8,43
4	8,94	8,76
5	8,31	7,9
6	7,16	6,57
7	15,63	15,57
8	13,08	13,08
9	12,37	11,93
10	15,44	14,77

From the table we note that the values obtained by the proposed algorithm are approximate to the values obtained by the planimeter. However, it should be borne in mind that planimeter measurements in this work were performed by an inexperienced operator, that is, the author of this paper.

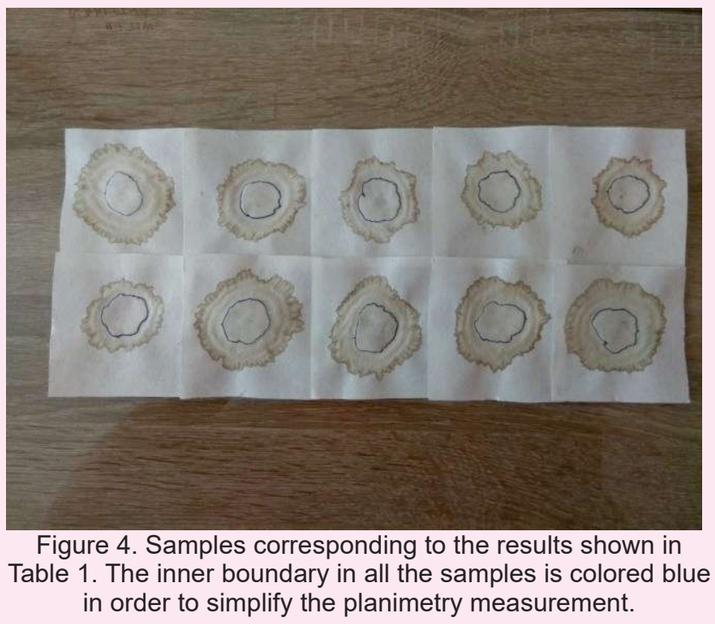

Figure 4. Samples corresponding to the results shown in Table 1. The inner boundary in all the samples is colored blue in order to simplify the planimetry measurement.

CONCLUSIONS

In this research, a novel system for measuring the water holding capacity of meat was designed and it’s functionality was experimentally verified. Experiments were conducted on ten different meat samples, and the obtained results were compared to a reference planimeter measurement method. It was shown that results obtained from both methods were in good agreement.

The developed acquisition system is consisted mostly of general purpose, low-cost components, and it provides multiple advantages over the planimeter method. The most important advantages include the measurement speed, simplicity, repeatability of results and no need for complicated operator training.

For further research, it is intended to implement the algorithm using free software libraries i.e. OpenCV, and make an application publically available to everyone. Dependance of results on the quality of the camera is to be quantified by using an industrial grade camera. It is also our intention to use the methods for analyze the measurement uncertainty of the proposed system. In the end, a 3D printer friendly test stand should be designed in order to further simplify the assembly of the whole acquisition system.

ACKNOWLEDGMENTS

The author would like to thank the team from The Faculty of Veterinary Medicine, University of Belgrade, as well as assistant professor dr Marko Barjaktarović and teaching assistant Petar Atanasijević for their work and support during this research.